Ohio Water Resources Center
Annual Technical Report
FY 2011

Introduction

Pursuant to the Water Resources Research Act of 1964, the Water Resources Center (WRC) is the federally-authorized and state-designated Water Resources Research Institute (WRRI) for the State of Ohio. The WRC was originally established in 1959 as part of the Engineering Experiment Station, College of Engineering, OSU, and conducted an extensive program of research on water and wastewater treatment processes. The Center continues to be administered through the College of Engineering and has maintained a tradition of placing special emphasis on encouraging and supporting research in the area of physical, chemical, and biological treatment processes for water and wastewater. The mission of WRC is to promote innovative, water-related research in the State of Ohio through research grant competitions, coordination of interdisciplinary research proposals, and educational outreach activities.

Research Program Introduction

In this reporting period we sponsored five new research projects from four different universities in Ohio totaling to $367,219 in research funding (direct and cost share). Seven students majoring in chemical engineering, environmental engineering, earth science, microbiology and other water related fields were supported. Two journal articles have been published and seven more are under development and/or review. Fifteen conference presentations were made during this report period based on the funded projects.

The funded research projects dealt with various Ohio Water Resources problems. For example, to better manage and monitor impaired water bodies Dion Dionysiou was investigating the development of a new Microcystin LR nanosensor and Chad Hammershcmidt evaluated the effects of alum addition to control algae bloom on lake communities. Some of the projects were not finalized yet and will be ongoing in the next year, such as Paula Mouser's investigation of wetland function in nitrogen cycle and methane emission and Ethan's Kubatko research on using Lake Erie waves as a source of renewable energy. In addition, Isabel Escobar progressed in developing new membranes for drinking water treatment and will continue her work next year as well.

A Hydraulic Modeling Framework for Producing Urban Flooding Maps in Zanesville, Ohio

Basic Information

Title:	A Hydraulic Modeling Framework for Producing Urban Flooding Maps in Zanesville, Ohio
Project Number:	2010OH150B
Start Date:	4/1/2010
End Date:	3/31/2011
Funding Source:	104B
Congressional District:	15
Research Category:	Climate and Hydrologic Processes
Focus Category:	Floods, Hydrology, Water Quantity
Descriptors:	
Principal Investigators:	Michael Durand, Konstantinos Andreadis

Publications

1. Lant, Jeremiah, 2011, A Hydraulic Modeling Framework for Producing Urban Flood Maps for Zanesville, Ohio, MS Thesis, Division of Geodetic Science, School of Earth Science, The Ohio State University, Columbus, Ohio, 50 pp.
2. Lant, Jeremiah, Michael Durand, and Doug Alsdorf, 2009, Hydrodynamic modeling of the Muskingum River near Zanesville, Ohio, paper presented at the Water Management Association of Ohio 2009 meeting, 4-5 November, Columbus, Ohio.
3. Lant, Jeremiah, Michael Durand, and Konstantinos Andreadis, Doug Alsdorf, 2010, Hydrodynamic Modeling of the Muskingum River near Zanesville, Ohio, paper presented at the American Society of Civil Engineers Environment and Water Resources Institute Watershed Management Conference meeting, 23-27 August, Madison, Wisconsin.
4. Lant, Jeremiah, Michael Durand, and Konstantinos Andreadis, Doug Alsdorf, 2010, A hydraulic modeling framework for producing urban flooding maps in Zanesville, Ohio, paper presented at the American Water Resources Association meeting, 1-4 November, Philadelphia, Pennsylvania.
5. Lant, Jeremiah, Michael Durand, and Konstantinos Andreadis, Doug Alsdorf, 2010, A hydraulic modeling framework for producing urban flooding maps in Zanesville, Ohio, paper presented at the Water Management Association of Ohio 2009 meeting, 17-18 November, Columbus, Ohio.
6. Lant, Jeremiah; Doug, Alsdorf, Michael, Durand, Kostas, Andreadis, 2012, A Hydraulic Modeling Framework for Producing Urban Flooding Maps in Zanesville, In The Ohio Water Table, Newsletter of Water Management Association of Ohio

FINAL REPORT TO USGS OHIO WATER RESOURCES CENTER

REPORT PERIOD: 1 APRIL 2010 – 31 MARCH 2011

Grant Title: A Hydraulic Modeling Framework for Producing Urban Flooding Maps in Zanesville, Ohio

Investigators: Michael Durand (PI) and Konstantinos Andreadis (Co-PI)

Department Address: School of Earth Sciences
125 South Oval Mall
275 Mendenhall Laboratory
The Ohio State University
Columbus, OH 43210
614-247-4835

PROBLEM AND RESEARCH OBJECTIVES

This project examines the flooding dynamics along the Muskingum River near the city of Zanesville, Ohio. Simulating various peak flood events using a hydrodynamic model will provide Muskingum County engineers with valuable information regarding inundated areas, extent, and effect on local communities for different flood events. The impact of various Muskingum River flood events, including the 100 year flood, on the urban environment in Zanesville, Ohio was studied. The project provides a useful hydraulic modeling framework that produces urban flooding maps for the city of Zanesville. These maps show how water surface elevations and water depths vary spatially and temporally, and will provide a more detailed picture of how flood waves move in urban environments. A hydrodynamic model called LISFLOOD-FP is used to simulate river flow and flooding. LISFLOOD-FP is a finite-difference flood inundation model that can accurately model 1D channel flow along with 2D floodplain flow. LISFLOOD-FP is a well-established hydrodynamic model that has been proven to properly simulate flood inundation for fluvial, coastal, and urban events.

The Federal Emergency Management Agency, FEMA, conducts flood insurance studies to identify a community's flood risk. The flood risk study is based upon statistical data for river flow, storm tides, hydrologic and hydraulic analyses, and rainfall and topographic surveys. The FEMA maps only provide a one-time snapshot of a flood, and do not describe the full extent of the flood event including the spatial and temporal variability of various flood events. Questions, such as the changes in flood inundation extent with time for the city of Zanesville, cannot be fully explored using the FEMA maps. It has been shown that accurate mapping of urban flooding events must take hydraulic connectivity and mass conservation into account. In other words, extending potential flood elevations along lines of equal elevation given a river elevation, the so-called "Planar GIS method," may be inadequate for characterizing urban flooding. An

alternative approach involves the simulation of hydraulic processes, which would control flooding and inundation patterns in downtown Zanesville given the FEMA 100 year Muskingum River main stem water surface elevation. Such an approach provides the framework, not only for producing dynamic maps of different frequency flood events for the city of Zanesville, but also evaluating the impacts of adding and/or removing structures or changing land use on urban flooding.

PERSONNEL

This work was done by Mr. Jeremiah Lant, and makes up his Master of Science thesis under Prof. Doug Alsdorf in the Geodetic Science division of the School of Earth Sciences. Mr. Lant defended his M.S. thesis on 24 May, 2011, and is currently finalizing the thesis document to be filed with the University.

METHODOLOGY

The objective of this research project was to create an urban flood study using a 2D hydrodynamic model, LISFLOOD-FP, for the city of Zanesville, Ohio. Flood inundation on a floodplain is controlled by the overlying topography and friction. Such flow is spatially complex, especially in the urban environment, with varying patterns of water velocity and depth that are two dimensional in space and dynamic in time. The creation of flood maps of water surface elevation and depth that provide a dynamic picture of flood inundation in the urban environment require a two dimensional hydrodynamic model. The LISFLOOD-FP hydrodynamic model is a two dimensional storage cell hydrodynamic model based on a finite difference scheme that can accurately simulate floodplain inundation in urban environments. The purpose of the LISFLOOD-FP code is to help improve understanding of flood hydraulics, flood inundation prediction, and flood risk assessment.

A 5 meter DEM derived from a 2.5 foot LIDAR dataset from the Ohio Geographically Referenced Information Program, OGRIP, was used. For an urban flooding scenario, building heights for the city of Zanesville, acquired from the Muskingum County engineers' office, were added onto the high resolution bare earth DEM using the same techniques to change the channel cell values. Muskingum River cross-sections are from 1934 Army Corps of Engineer maps. These maps were acquired from the Ohio Department of Natural Resources. Average bed elevations at each data cross-section were computed within the river channels. From the Federal Insurance Study (FIS) conducted for the city of Zanesville, FEMA defined the 100 year flood discharge along the Muskingum River near the city of Zanesville, Ohio to be 68,000 cubic feet per second, and the 100 year flood discharge along the Licking River below the Dillon Dam to be 7,200 cubic feet per second. To show the spatial and temporal evolution of a possible 100 year flood for Zanesville, hydrographs from the USGS for the Muskingum River and Licking River with peaks nearest the FEMA defined 100 year flood discharge were found and used. These hydrographs consisted of a twelve day flood event. Each hydrograph was linearly scaled to match the respective FEMA peak.

PRINCIPAL FINDINGS AND SIGNIFICANCE

The study produced a model framework that yields dynamic urban flood maps of Zanesville. The framework was built around simulating a FEMA-defined 100 year flood. Modeling efforts demonstrate similar flood profiles and water surface elevations when compared to FEMA (Figure 1). The flood maps show how a 100 year flood wave evolves over time.

A comparison study was made between 1D HEC-RAS and 2D LISFLOOD-FP models. Results have shown that both models produce comparable water surface elevations within the river channel and on the floodplain (Figure 2). With the model framework built, simulations of other flood events can be completed. Since the heart of Zanesville is fairly protected from the 100 year flood, an investigation into the amount of discharge needed to reach downtown Zanesville was conducted. It was found that a massive flood wave, over 100,000 cfs, might be needed to inundate the entire downtown area of Zanesville (Figure 3). A flowrate of this magnitude is approximately 50% greater than the 100 year flood utilized in the FEMA study. Although highly improbable, the dynamic mapping of this flood event provides a deeper understanding of how flood waters could move in the urban environment. A flood event case with data from USGS Streamstats was completed to analyze how a flood might impact Zanesville without the influence of any flood control structures. Without such flood control structures, Zanesville would be seriously inundated if a 100 year flood occurred.

The model framework built in this study allows the sensitivity of climate change and urbanization on the FEMA 100 year water surface elevations and extent to be analyzed. A follow-on study could, ideally, use this framework to further explore changing flooding patterns in an urban environment due to dam sedimentation, land use and land cover change, climate change, and urbanization. This study of urban flooding on the Muskingum River also represents an opportunity to more fully understand the performance of the upcoming Surface Water Ocean Topography Mission, SWOT (http://swot.jpl.nasa.gov), over modest sized rivers in an urban environment. The SWOT satellite will have the capability of measuring temporal and spatial changes in water surface elevations and inundated areas for fresh water bodies around the world. From these measurements, depth and discharge along much of the Muskingum River can be extracted and used in hydrodynamic models like LISFLOOD-FP. Better knowledge of discharge on the Muskingum River will provide a valuable insight into how floods travel through the floodplain and affect the urban environment.

CONCLUSION

Mr. Lant has completed the construction of the hydraulic framework for testing flooding scenarios in Zanesville. Several example scenarios were presented here. The work formed the bulk of Mr. Lant's M.S. thesis, and was presented at four conferences, including ASCE and AWRA. We plan to submit a full-length journal manuscript on this work in the upcoming months.

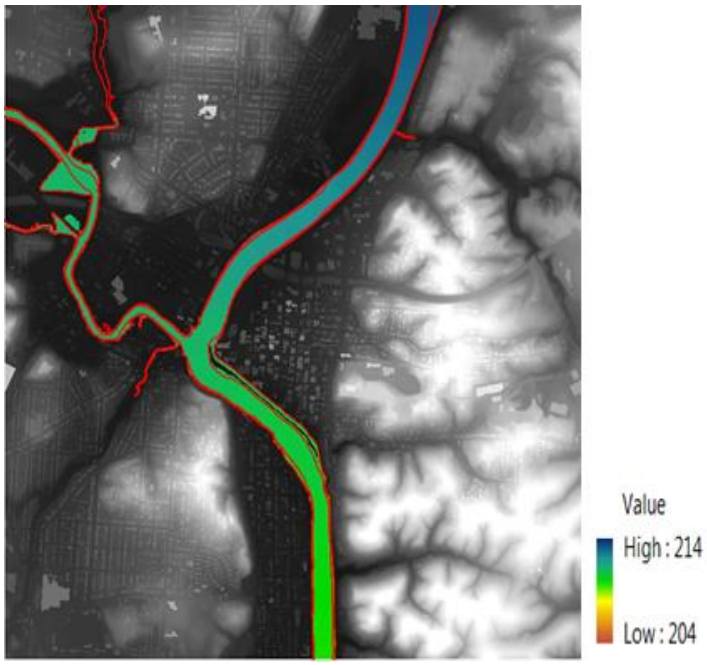

Figure 1. LISFLOOD-FP flood extent shows good agreement with FEMA 100 year flood extent (red). Water surface elevation values are in meters.

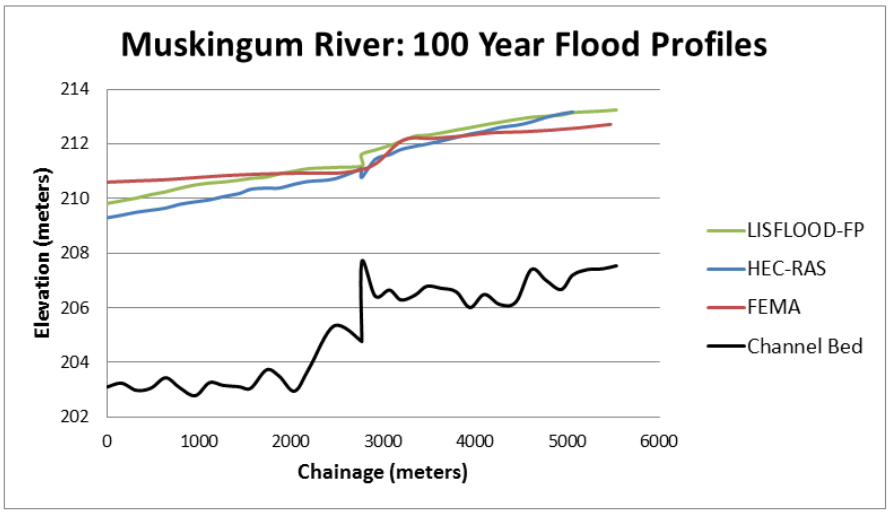

Figure 2. Comparison of water surface profiles.

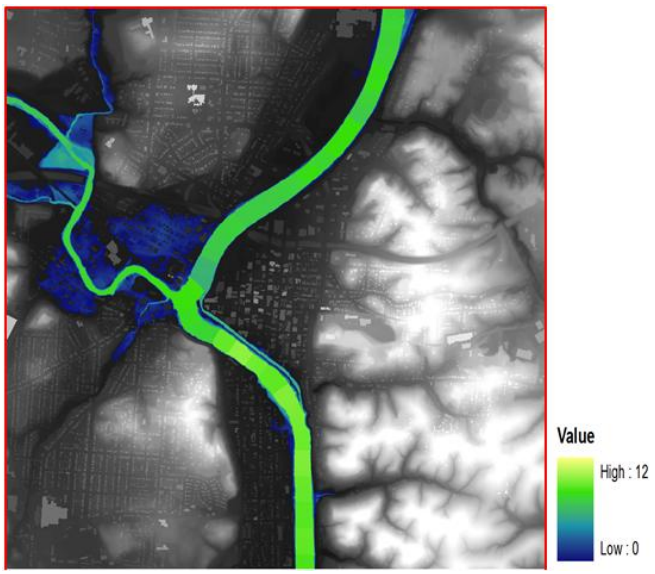

Figure 3. Water depth map of increasing FEMA flood peak by 50%. Water depths are in meters. The city of Zanesville is inundated with water depths ranging from 0.1 meters to 1.5 meters.

MASTER OF SCIENCE THESIS

Lant, Jeremiah, 2011, A Hydraulic Modeling Framework for Producing Urban Flood Maps for Zanesville, Ohio, MS Thesis, Division of Geodetic Science, School of Earth Science, The Ohio State University, Columbus, Ohio, 50 pp.

CONFERENCE PRESENTATIONS

Lant, Jeremiah, Michael Durand, and Doug Alsdorf, 2009, Hydrodynamic modeling of the Muskingum River near Zanesville, Ohio, paper presented at the Water Management Association of Ohio 2009 meeting, 4-5 November, Columbus, Ohio.

Lant, Jeremiah, Michael Durand, and Konstantinos Andreadis, Doug Alsdorf, 2010, Hydrodynamic Modeling of the Muskingum River near Zanesville, Ohio, paper presented at the American Society of Civil Engineers Environment and Water Resources Institute Watershed Management Conference meeting, 23-27 August, Madison, Wisconsin.

Lant, Jeremiah, Michael Durand, and Konstantinos Andreadis, Doug Alsdorf, 2010, A hydraulic modeling framework for producing urban flooding maps in Zanesville, Ohio, paper presented at the American Water Resources Association meeting, 1-4 November, Philadelphia, Pennsylvania.

Lant, Jeremiah, Michael Durand, and Konstantinos Andreadis, Doug Alsdorf, 2010, A hydraulic modeling framework for producing urban flooding maps in Zanesville, Ohio, paper presented at the Water Management Association of Ohio 2009 meeting, 17-18 November, Columbus, Ohio.

The Constructed Wetland Dilemma: Nitrogen Removal at the Expense of Methane Generation?

Basic Information

Title:	The Constructed Wetland Dilemma: Nitrogen Removal at the Expense of Methane Generation?
Project Number:	2011OH205B
Start Date:	3/1/2011
End Date:	2/28/2013
Funding Source:	104B
Congressional District:	12
Research Category:	Climate and Hydrologic Processes
Focus Category:	Nutrients, Wetlands, Climatological Processes
Descriptors:	
Principal Investigators:	Paula J Mouser, Gil Bohrer

Publications

1. Mouser, Paula, Michael Brooker, William Mitsch, Gil Bohrer, 2012, Factors Influencing Microbial Gas Production Rates in a Constructed Wetland Ecosystem. Oral Presentation, 5/2012, In 30th AMS Conference on Agricultural and Forest Meteorology, Boston, MA.
2. Bohrer, Gil; Liel Naor-Azrieli; Scott Mesi; Paula Mouser; K Stefanik; KV Schafer; William Mitsch, 2012, Determining the meteorological forcing that affect seasonal and diurnal dynamics of methane emissions at a constructed urban wetland in Ohio. Oral Presentation, 5/2012, In 30th AMS Conference on Agricultural and Forest Meteorology, Boston, MA.
3. Shafer, KV; Gil Bohrer, Liel Naor-Azrieli, Paula Mouser, William Mitch, M Wu, 2011, Temporal Dynamics of Methane Fluxes in Temperate Urban Wetlands, Poster Presentation B12C-05, 12/2011, In American Geophysical Annual Meeting, San Francisco, CA.
4. Naor-Azrieli, Liel; Gil Bohrer, William Mitsch, 2011, Collaborative research: Greenhouse gas balance of urban temperate wetlands. Oral presentation, 5/2011, In Annual Meeting of the American Ecological Engineering Society, Ashville, NC.

Progress Report 2011-2012

Contract Information

Title	The Constructed Wetland Dilemma: Nitrogen Removal at the Expense of Methane Generation?
Project Number	2011OH205B
Start Date	3/1/2011
End Date	2/28/2013
Focus Category	Nitrate Contamination, Wetlands, Ecology
Keywords	Bacteria, Biotechnology, Nitrate Removal, Methane Flux, Constructed Wetlands
Lead Institute	The Ohio State University
Principal Investigators	Paula Mouser, Gil Bohrer

Abstract

Constructed wetlands provide a valuable ecosystem service by sequestering carbon dioxide from the atmosphere and serving as a sink for atmospheric nitrogen export. Unfortunately, carbon sequestration and denitrification in wetlands come with the tradeoff of increased production of methane – another more potent green house gas. Methane is produced by methanogenic archaea that thrive in chemically reduced, anaerobic zones of the wetland. Dinitrogen export, on the other hand, is thought to occur under suboxic conditions by denitrifying bacteria. Few studies have examined the *in situ* rates of metabolic activity for dominant microorganisms driving these processes or systematically evaluated the key factors controlling their metabolic rates in wetland environments. This research evaluates how three environmental factors: temperature, wetland biome, and redox environment relate to microbial ecology and *in situ* gas production in a constructed wetland ecosystem located in central Ohio. Microbial measurements provide information about instantaneous fluxes under differing environmental conditions but are not necessarily representative of long-term fluxes that may be quantified using surface chamber measurements or atmospheric eddy-covariance methods. The objective of this research is to develop upper limit estimates for *in situ* microbial gas production rates under differing environmental conditions so that we may better understand how they relate to spatiotemporal surface and plot-scale emission rates also measured at the site.

Problem

Sources of fixed nitrogen (N) are essential for the growth of all biological organisms, and agriculture is dependent on nitrogen supply for fertilization. When present at elevated levels in drinking water, however, certain nitrogen species present significant health risks to humans including blue baby syndrome, enlarged thyroids, and increased risk of certain cancers. It can also contribute to hypoxic conditions in certain lakes and coastal environments. For example, eutrophication in the Gulf of Mexico and the Great Lakes region has largely been attributed to imbalances between nitrogen fertilizer application and crop uptake, and precipitation runoff from livestock feed lots in Ohio and other mid-West states. Limiting the transport of nitrogen from its source is therefore key to protecting Ohio's water resources and lowering health risks and environmental impacts to nearby regions.

One suggested method for reducing nitrogen export is the use of constructed wetlands or riparian

buffer zones between discharge points and water bodies to transform aquatic anthropogenic N inputs, such as nitrate, to a gaseous form released to the atmosphere, thereby reducing its transport to potential receptors. Unfortunately, denitrification in wetlands comes with the tradeoff of increased Green House Gas (GHG) production. In order to allow development of wetlands as a solution for N removal without concerns of GHG production, it is critical to understand what factors control methane production and how emissions relate to wetland aquatic conditions. **The objectives of this research are to: 1) elucidate the environmental factors influencing the *in situ* metabolic condition of denitrifiers and methanogens in a constructed wetland environment, and 2) link N removal and methane production rates to GHG budgets.** Progress to date on these objectives includes the following methods and preliminary findings.

Methodology

During 2011 we performed preliminary laboratory experiments and molecular work to refine our techniques and understanding of factors influencing field-scale processes at the ORWRC. Soil cores were collected from three locations at the wetland, including: 1) an area consistently inundated with standing water "open water", 2) a saturated area dominated by macrophyte vegetation "typha", and 3) a less-saturated area topographically upland of the wetland "upland". We have expanded the automated on-line monitoring setup at the wetland to measure soil temperatures in these three environments at two depths (5, and 30 cm) at the two wetlands. This was done by adding a sensor network with 14 soil temperature probes. These measurements are on going once per minute and are recorded with all other meteorological measurements and CO_2 and methane flux measurements at the wetland meteorological station. Microcosms were constructed in 150 ml serum bottles for each of the three soil types (~40 g) with water collected from the inundated area (~80 ml) and stored under anaerobic conditions for approximately 2.5 months. Bottles were incubated at 20ºC or 30ºC to assess the rate of methane generation as a function of soil type and temperature.

One of our first tasks was to evaluate whether our existing molecular methods could be used in this application, and then develop a database of microbial community information for designing primers targeting methanogenesis and denitrification to address the questions posed in this proposal. To accomplish this we extracted genomic DNA from microcosm sediments; tested the specificity of primers amplifying two 16S rRNA genes targeting bacteria and archaea; sequenced microbial members belonging to these domains; and generated community profiles using terminal restriction fragment length polymorphism (T-RFLP) from the different soils. These DNA sequences and community profiles will be used to generate a clone library to design primers for quantification of *nirS* and *mcrA* levels.

We are currently preparing for the collection of cores and concurrent installation of shallow groundwater wells at the ORWRC in early June. The wells will be installed into the inundated, macrophyte, and upland areas described above. Groundwater will be collected from several depths in the nested wells (aerobic, suboxic and anaerobic) for assessment of metabolic activity of denitrifiers and methanogens and solution biogeochemistry during the summer and fall months.

Preliminary Findings

Initial microcosm results yielded useful data for refining our techniques and understanding of the wetland system. We observed that an increase of 10ºC incubation temperature resulted in a 2- to 24- fold increase in methane generation for these soils, with the open water having the smallest overall increase and the upland having the largest overall increase in generation as a result of temperature. Average generation rates are consistent with rates measured at the surface of the wetland during spring and summer by Altor and Mitsch, 2008.

Over a period of 77 days, we found that average methane generation rates in the open water soils at 30ºC were more than 3-fold higher than those produced from both the upland and typha soils at this same temperature (Figure 1). At 20ºC, these differences were even more apparent, with the open water soils producing between 4- and 40- times the methane of the typha and upland soils (Figure 1). Nitrate and nitrite-N concentrations were below detection throughout the experiment. These findings suggest that the wetland biome has a significant effect on methane generation rates and that this effect is dampened as temperature increases, possibly as a result of methanogens being able to out compete other microorganisms for resources.

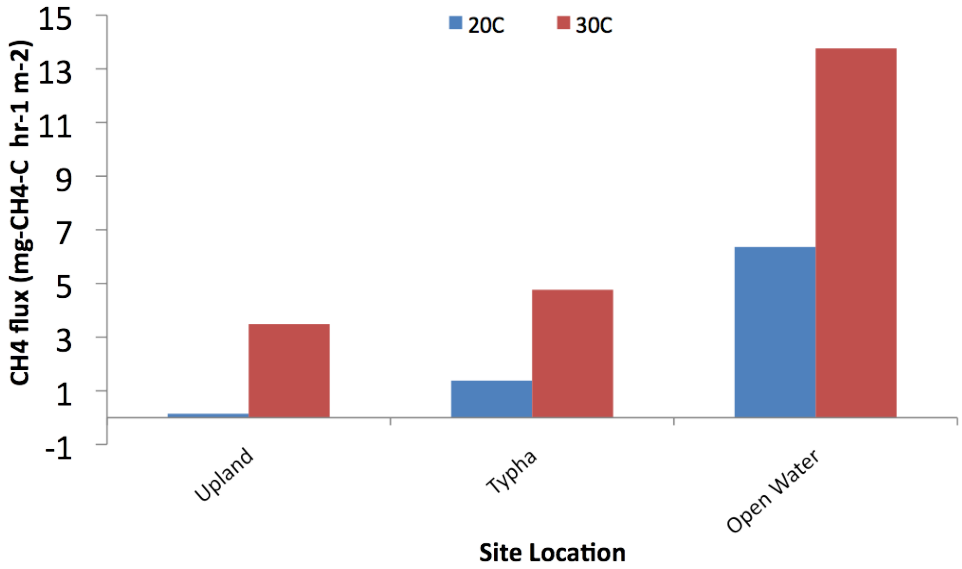

Figure 1. Average methane generation rates in microcosm studies for three different soil types colleted at the wetland.

Preliminary microbial community profiling suggest that methane-producing microorganisms were in higher abundance in open water soils. Methanogens made up approximately 15% of the Archaeal community in open water microcosms while they were detected at less 12% in upland and typha soils. Ecological indices indicate that the upland microcosms held higher bacterial and Archaeal diversity than typha and open water soils, supporting the observation that methanogens dominate under conditions when they can out compete other microbes. Further community profiling and DNA sequence analysis will be used to identify microbes in higher abundance in these soils for developing primers targeting *mcrA* and *nirS* genes.

Significance

Our findings suggest that a location within a wetland, or its biome, plays a significant role in the rate of methane generation across a site. This location effect appears to be heightened at lower temperatures (20ºC) possibly due to slower growth rates and the ability of a diverse pool of microbes to compete for resources. Methanogens may have means to out compete others at higher temperatures, thus producing overall higher rates of methane from varying soils.

Publications/Proceedings/Conference Presentations

1. Mouser, PJ, Brooker, M, Mitsch, W, and Bohrer, G. (2012), Factors Influencing Microbial Gas Production Rates in a Constructed Wetland Ecosystem. Oral Presentation, 5/2012. *30th AMS Conference on Agricultural and Forest Meteorology, Boston, MA*.

2. Bohrer, G, Naor-Azieli, L, Mesi, S, Mouser, PJ, Stefanik, K, Schafer, KVR, and Mitsch, W (2012), Determining the meteorological forcing that affect seasonal and diurnal dynamics of methane emissions at a constructed urban wetland in Ohio. Oral Presentation, 5/2012. *30th AMS Conference on Agricultural and Forest Meteorology, Boston, MA*.

3. Shafer, KV, Bohrer, G, Naor, L, Mouser, PJ, Mitch, WJ, Wu, M (2011), Temporal Dynamics of Methane Fluxes in Temperate Urban Wetlands, Poster Presentation B12C-05, 12/2011. *American Geophysical Annual Meeting, San Francisco, CA*.

4. Naor-Azrieli, L, Bohrer G, Mitsch W. (2011), Collaborative research: Greenhouse gas balance of urban temperate wetlands. Oral presentation 5/2011. *Annual Meeting of the American Ecological Engineering Society*, Ashville, NC.

Students Supported By Project

1. Michael Brooker – M.S. student in Environmental Science Graduate Program (June 2011-current).

Awards or Achievements

None to date.

Does Alum Addition Affect Benthic Communities and Metal and Nutrient Cycling? A Case Study from Grand Lake St. Marys, Ohio

Basic Information

Title:	Does Alum Addition Affect Benthic Communities and Metal and Nutrient Cycling? A Case Study from Grand Lake St. Marys, Ohio
Project Number:	2011OH207B
Start Date:	3/1/2011
End Date:	2/29/2012
Funding Source:	104B
Congressional District:	7
Research Category:	Water Quality
Focus Category:	Ecology, Conservation, Water Quality
Descriptors:	
Principal Investigators:	Chad Hammerschmidt, Amy Burgin, Geraldine Nogaro

Publications

1. Nogaro G., AJ Burgin, V Schoepfer, M Konkler, K Bowman, CR Hammerschmidt. Alum treatment affects metal and biogeochemical cycling in hypereutrophic lake ecosystem. In preparation for Journal of Environmental Quality
2. Nogaro G, AJ Burgin, A Taylor, M Konkler, V Schoepfer, CR Hammerschmidt. Can alum prevent harmful algal blooms and restore water quality in Grand Lake St. Mary s, Ohio? In preparation for Journal of Environmental Quality
3. Nogaro G., AJ Burgin, A Taylor, D Marsh, K Lam, CR Hammerschmidt. Interactions between alum addition and invertebrate bioturbation on nutrient and metal releases in eutrophic lake sediments. In preparation for Freshwater Biology.
4. Taylor A, CR Hammerschmidt, AJ Burgin, G Nogaro. Mass balance for phosphorous in eutrophic Grand Lake St. Mary s, Ohio. In preparation for Water Research.
5. Nogaro G, AJ Burgin, V Schoepfer, M Konkler, K Bowman, CR Hammerschmidt. Alum treatment affects metal and biogeochemical cycling in hypereutrophic lake ecosystem. In preparation for Journal of Environmental Quality
6. Taylor A; Geraldine Nogaro, AJ Burgin, Chad Hammerschmidt, 2012, Phosphorus budget and benthic flux in eutrophic Grand Lake Saint Mary s, Ohio. Geological Society of America North-Central Section, 46th Annual Meeting, April 23 24 2012, Dayton OH
7. Nogaro Geraldine; AJ Burgin, Chad Hammerschmidt, 2012, Influence of alum addition on metal and nutrient cycling in Grand Lake Saint Mary s, Ohio, In Environmental Science Graduate Program s spring seminar series, Ohio State University, April 6 2012, Columbus OH
8. Nogaro Geraldine, Chad Hammerschmidt, AJ Burgin, 2011, Alum influence on metal and nutrient cycling and benthic communities in a shallow eutrophic lake, In Annis water Resources Institute seminar series, Grand Valley State University, July 22 2011, Muskegon MI
9. Nogaro Geraldine; Chad Hammerschmidt, AJ Burgin, 2011, Influence of alum addition on metal and nutrient cycling in Grand Lake Saint Mary s, Ohio, In North American Benthological Society

(NABS) meeting, May 22-26 2011, Providence RI

Annual Report

Does Alum Addition Affect Benthic Communities and Metal and Nutrient Cycling? A Case Study from Grand Lake St. Marys, Ohio

Chad R. Hammerschmidt, Amy J. Burgin, G. Nogaro

Table of contents

1. SUMMARY

Grand Lake Saint Mary's (GLSM) experiences severe eutrophication due to high loadings of phosphorus (P) and associated blooms of harmful cyanobacteria. The decline of the lake's water quality has caused a significant loss to the regional economy. The Ohio EPA experimentally added aluminum sulfate (alum) to GLSM to chemically treat P, which can reach 1,000 µg/L. Our study focuses on the ecological consequences of alum additions on benthic microbial and invertebrate communities, as well as associated nutrient and metal cycling in the lake. Our approach combines field sampling of non-alum amended sites and alum-amended sites on GLSM with a mesocosm experiment that manipulated bioturbating organisms and alum addition. Water and sediment samples from the field and mesocosm experiment were analyzed for physicochemical parameters, dissolved ions, dissolved and particulate metals, and microbial activities. Our results indicate that alum addition can greatly increase dissolved aluminum in surface and pore waters compared to the non-alum amended sites, likely beyond toxicity thresholds for some organisms. Alum treatment also increased sulfate in surface and pore waters. The increase of metals and alternative electron acceptors may feedback to alter microbial community dynamics and invertebrate communities. Our results showed that the presence of bioturbating fauna can reduce the effectiveness of alum addition by stimulating phosphate releases from the sediment to the water column. Results from this work will enhance our understanding of the ecological consequences of alum additions in GLSM and, in general, eutrophic freshwater ecosystems elsewhere.

2. PROBLEM AND RESEARCH OBJECTIVES

Excessive nutrient loadings to aquatic ecosystems cause eutrophication, a process associated with increased primary production and simplification of biodiversity (Smith et al., 1999). GLSM is Ohio's largest inland lake at 52.4 km^2, with a maximum depth of about 2 m and a watershed of 230 km^2 (Fig. 1). Cultural eutrophication due to agriculture (cropland) and livestock operations in 90% of GLSM's watershed has resulted in excessive P loadings to the lake and subsequent blooms of toxic blue green algae (Hoorman et al., 2008). A lake classified as being eutrophic typically has between 25–50 µg total P L^{-1}; surface water of GLSM has contained in excess of 1,000 µg L^{-1} of P during the summer (Hoorman et al., 2008).

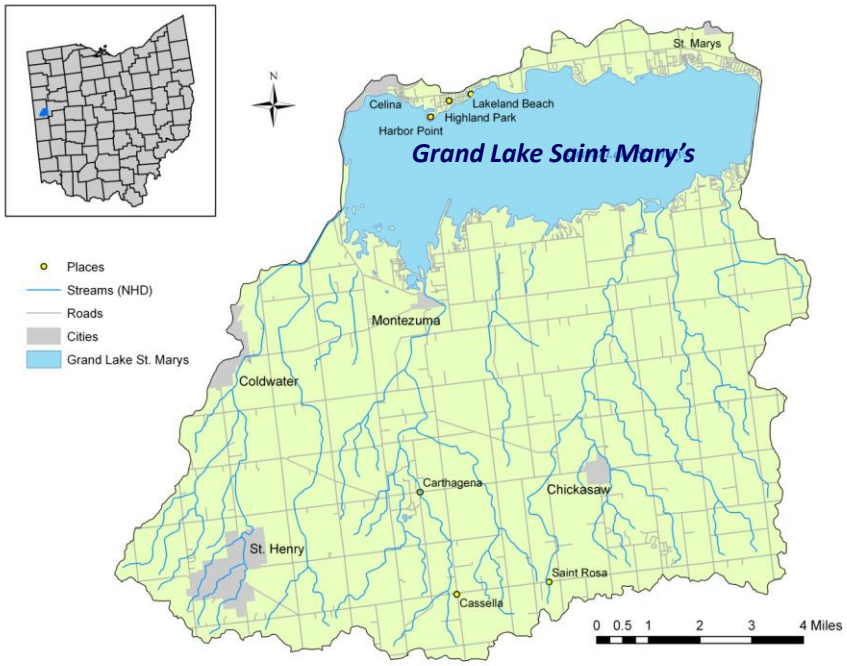

Fig. 1 Grand lake Saint Mary's watershed

Eutrophication has ecological and economic consequences. Decomposition of the produced biomass results in depleted levels of dissolved oxygen, which can lead to fish kills such as those that occurred in GLSM on June 28 and 29, 2009 (Allen, 2009). Furthermore, blooms of such bacteria can release high levels of neuro- and hepatotoxins to the water, which led the Ohio Environmental Protection Agency (OH EPA) to declare a "no contact" rule for GLSM during the summers of 2009 and 2010: nine people became sick and three dogs died after contact with the lake (Barlow, 2010). Because GLSM is a popular recreation lake for boating, fishing, and swimming, the decline of the lake's water quality also has caused a significant economic loss to local businesses and the overall livelihood of the region (Barlow, 2010). Local home and business owners have pressured state leaders to find short-term solutions to reduce cyanobacteria blooms in GLSM. Management of eutrophication due to high P loadings is difficult because P, unlike nitrogen, does not have an atmospheric component, and is therefore retained completely in the system unless removed physically. Phosphorus can be removed from the lake only by discharge (water or sediment removal) or sorbing permanently to the sediments (Carpenter et al., 1999). Addition of aluminum sulfate (alum) to GLSM has been proposed by the OH EPA and the OH Department of Agriculture (DoA), together with the environmental consulting group TetraTech, as a short-term treatment to decrease P levels and combat the harmful algal blooms.

Alum ($Al_2(SO_4)_3 \bullet 14H_2O$) can be used to chemically treat P-enriched eutrophic lakes. When added to water, alum hydrolyzes to form an amorphous floc of $Al(OH)_3(s)$ ($pK_{sp} = 32$) that has a high adsorption affinity for P (Huang et al., 2002) and can react with PO_4^{3-} to form insoluble $AlPO_4(s)$ ($pK_{sp} = 21$). The primary goal of alum additions is to form an $Al(OH)_3(s)$ floc on the sediment surface that minimizes P release to the water column. Although alum has been used to treat excess P in lakes worldwide since the 1970's, the solubility, chemistry, and toxicity dissolved Al after an alum treatment are still not well known (Kennedy and Cooke, 1982; Gensemer and Playle, 1999). Water pH plays a key role in Al chemical phases after an alum treatment because $Al(OH)_4^-$ dominates at high pH, $Al(OH)_3$ between 6 and 8 and free Al^{3+} at low pH (Kennedy and Cooke, 1982). Berkowitz et al. (2005) showed in a laboratory study that alum addition to water samples resulted in a rapid initial pH decrease followed by a gradual recovery and an increase of dissolved Al concentrations up to 2500 µg L^{-1} after 17 days and then a decrease to < 250 µg L^{-1} after 150 days. Importantly, and after treatment with alum, there was a 35-d period in Lake Elsinore when aluminum exceeded 1000 µg L^{-1} at a pH of about 8.5 (Berkowitz et al., 2005)—conditions that can cause short-term toxicity (Gensemer and Playle, 1999). Another consequence of alum additions is an increased amount of sulfate (SO_4^{2-}) in the system. Sulfate is a desirable alternative electron acceptor for anaerobic microbial metabolism, and increasing SO_4^{2-} has been associated with increased SO_4^{2-} reduction rates (Vile et al., 2003; Weston et al., 2006). SO_4^{2-} reduction results in sulfide (S^{2-}), which is toxic to benthic organisms and interferes with many sensitive biomolecules, including enzymes (Wang and Chapman, 1999).

This study focuses on the ecological consequences of alum additions on benthic microbial and invertebrate communities, as well as associated nutrient and metal cycling. We ask the *overarching question*: ***How does the addition of alum affect invertebrate bioturbation, microbial nutrient processing and metal cycling in Ohio's GLSM?***

From this overarching question, we have tested three specific hypotheses (H_1–H_3) with an approach that combined field sampling of the already extant alum addition sites on GLSM with a mesocosm experiment that manipulated bioturbating organisms and alum addition levels.

H_1: Alum additions increase Al concentrations in the water and near-surface sediments of GLSM.

H_2: Alum additions increase sulfate levels in GLSM, which in turn will enhance microbial sulfate reduction rates and generation of sulfide.

H_3: Alum additions will decrease microbial activity and invertebrate bioturbation in the sediment, which, in turn, will affect nutrient and metal cycling of GLSM.

3. FIELD SAMPLING IN NOVEMBER 2010

3.1. Methodology

In September 2010, the OH EPA conducted a pilot study to examine the efficacy of alum additions on planktonic growth in three small bays of GLSM: Harmon's Channel, Otterbein Channel No.1 and West Bank Marina. We used these alum test locations, with matched reference sites, to investigate the effects of alum treatment on metal and nutrient cycling in surface waters and lake sediments (Fig. 2). The dosage of alum was 31.6 mg/L as alum and sodium aluminate (used as a buffer), which was applied on September 20, 2010 in the three shallow bays of GLSM (Table 2). The total cost of such alum treatment was $61,500 (TetraTech, 2010).

In November 11, 2010 (i.e., about 3 weeks after the alum addition by the OH EPA), we performed *in situ* measurements and sampling of water and sediment at the alum-amended sites and matched reference sites (i.e., with no alum addition) of Harmon, Otterbein and West Bank Marina locations of GLSM (Fig. 2). We worked in collaboration with Dr. Robert Hiskey, Associate Professor of Biological Sciences at Wright State University – Lake Campus. Dr. Hiskey has offered his boat and equipment at the Lake Campus marina to collect water and sediment samples on GLSM. Surface water and sediments from three alum treatment and reference sites were analyzed for physicochemical parameters, dissolved ions, dissolved and particulate metals, and microbial activities. We expected that alum additions would increase Al concentrations in the water and near-surface sediments of GLSM. We also expected that alum additions would increase sulfate levels in GLSM, which in turn will enhance microbial sulfate reduction rates and generation of sulfide.

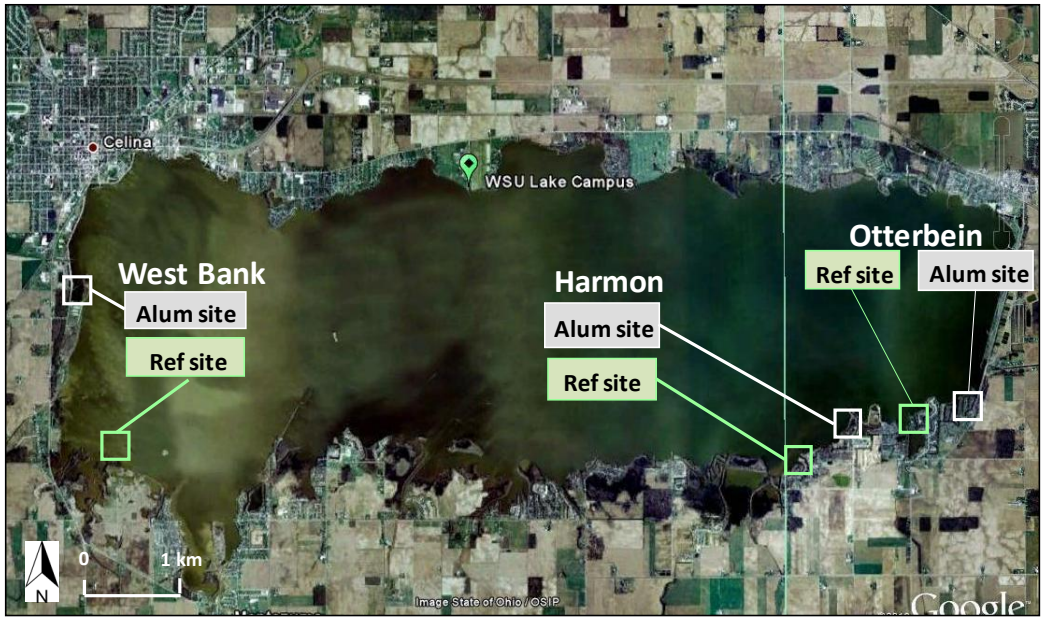

Fig. 2. Map of the aluminum sulfate addition (alum) and reference (ref) sites of Harmon, Otterbein and West Bank Marina locations in Ohio's Grand Lake Saint Mary's.

Table 1. Characteristics of the three demonstration project locations (TetraTech, 2010)

Site	Area (m^2)	Dosage (kg Al)	Depth (m)
Harmon	53,000	2,012	1.2
Otterbein	31,000	1,449	1.5
West Bank	36,000	2,083	2.0

At each site, surface water samples were analyzed for dissolved oxygen, pH, temperature, specific conductance, chlorophyll, redox potential, turbidity, total suspended solids (TSS), dissolved and particulate inorganic and total phosphorus, dissolved nitrate, nitrite, ammonium, dissolved sulfate, and organic carbon with standard methods (APHA et al., 1995). We also measured dissolved and particulate aluminum and other biologically active metals that may be affected by alum addition, including copper, nickel, zinc, cobalt, lead, manganese, and iron. Intact, undisturbed sediment cores were collected and sectioned into 0–1, 1–2, 2–3, and 3–4 cm depth horizons and pore water extracted by vacuum filtration (Hammerschmidt et al., 2004). Filtered water also was measured for metals, sulfide, phosphate, nitrate, nitrite, ammonium, and organic carbon. Water and sediment was sampled with trace-metal clean techniques (Gill and Fitzgerald, 1987) and transported promptly to Wright State University for processing and analysis. Sediments also were sampled to quantify microbial activities (hydrolytic and dehydrogenase) as well as invertebrate density and species richness. Hydrolytic and dehydrogenase activities indicate aerobic enzymatic and respiratory microbial activities, respectively.

3.2. Principal findings

Our results indicate that alum-treated locations experienced an increase of pH and a decrease of turbidity, chlorophyll and redox potential in the surface water compared to the reference sites (Table 2). The increase of pH can be attributed to a buffer (i.e., sodium aluminate) added with the acidic alum, whereas reductions of turbidity, chlorophyll, and redox potential are consistent with reduced primary production.

Table 2. *In-situ* measurements in the surface water of the reference (i.e., Ref) and the alum-treated (i.e., Alum) sites of Grand Lake Saint Mary's in November 11, 2010

	Harmon		**Otterbein**		**West Bank**	
	Ref	Alum	Ref	Alum	Ref	Alum
pH	7.98	8.22	8.17	8.81	8.84	9.79
Turbidity (NTU)	43.5	26.5	48.7	26.0	8.5	7.9
Chlorophyll (ug/L)	11.7	5.9	14.1	6.7	11.7	5.9
Redox potential (mV)	223	210	249	158	217	160

As expected, alum additions decreased total suspended solids (TSS) concentrations in surface water (Fig. 3A). Soluble reactive phosphorus (SRP) also was reduced substantially at two of the three test locations (Fig. 3B). SRP concentrations were relatively low (7–40 μL^{-1}) because it is the most available form of P for biological uptake and the sampling was performed in November (i.e., end of algae growing season) in small embayments.

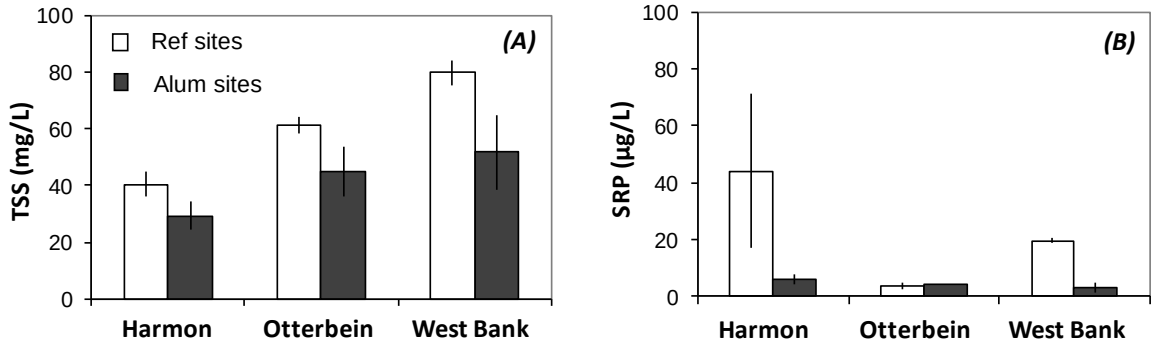

Fig. 3. Concentrations of (A) total suspended solids (TSS) and (B) soluble reactive phosphorus (SRP) in the surface water of the reference (ref) and alum-amended (alum) sites of Harmon, Otterbein and West Bank Marina locations in GLSM (mean ± 1 SE, *n=3*).

Moreover, the alum treatment decreased the dissolved total P (Fig. 4A) and particulate total P (Fig. 4B) in comparison with the reference sites. However, and even after the treatment, the lake surface water was still highly eutrophic because concentration of dissolved + particulate TP remained greater than 100 ug/L in each of the three bayss (Fig. 4).

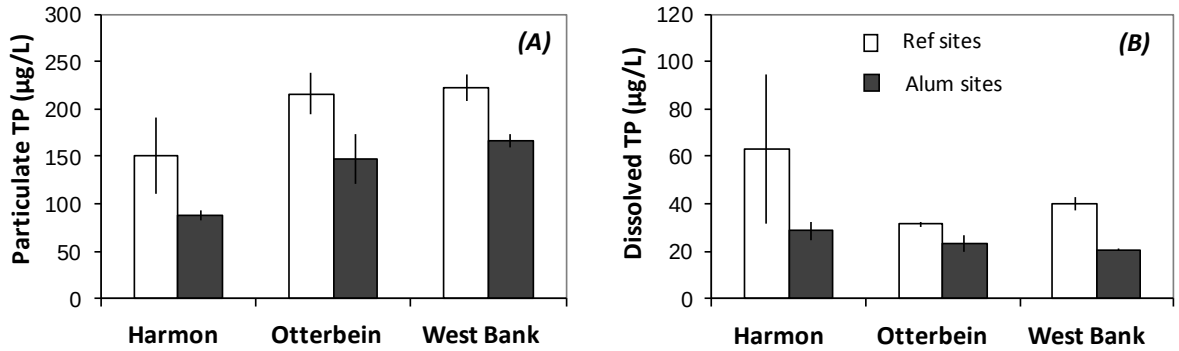

Fig. 4. Concentrations of (A) dissolved total phosphorus (dissolved TP) and (B) particulate total phosphorus (particulate TP) in the surface water of the reference (ref) and alum-amended (alum) sites of Harmon, Otterbein and West Bank Marina locations in GLSM (mean ± 1 SE, *n=3*).

A primary concern with alum additions is potential and unintentional toxicological effects of aluminum (Al) on biotic communities. Al has relatively simple chemical speciation in water, existing principally as free Al^{3+} at pH < 5, insoluble $Al(OH)_3(s)$ and $Al(OH)_3^0$ at pH between about 5 and 9, and dissolved $Al(OH)_4^-$ at pH > ~9. Hence, differences and changes in pH can affect the solubility and speciation of Al. Our preliminary results indicate high levels of Al in filtered (0.45 µm) surface and pore waters of Otterbein and West Bank alum test locations compared to the reference sites (Fig. 5)—mean levels of Al in filtered surface water were 340 and 2030 µg L^{-1}, respectively. These levels are orders of magnitude greater than those predicted from solubility product estimates of $AlPO_4$ and $Al(OH)_3(s)$ at pH 7–10, which suggests that either natural organic ligands may promote dissolution of the Al minerals or that a substantial fraction of the Al is associated with colloids. Such levels of Al are associated commonly with toxicity to many species of phytoplankton, macrophyte, aquatic invertebrate and fish (Gensemer and Playle, 1999).

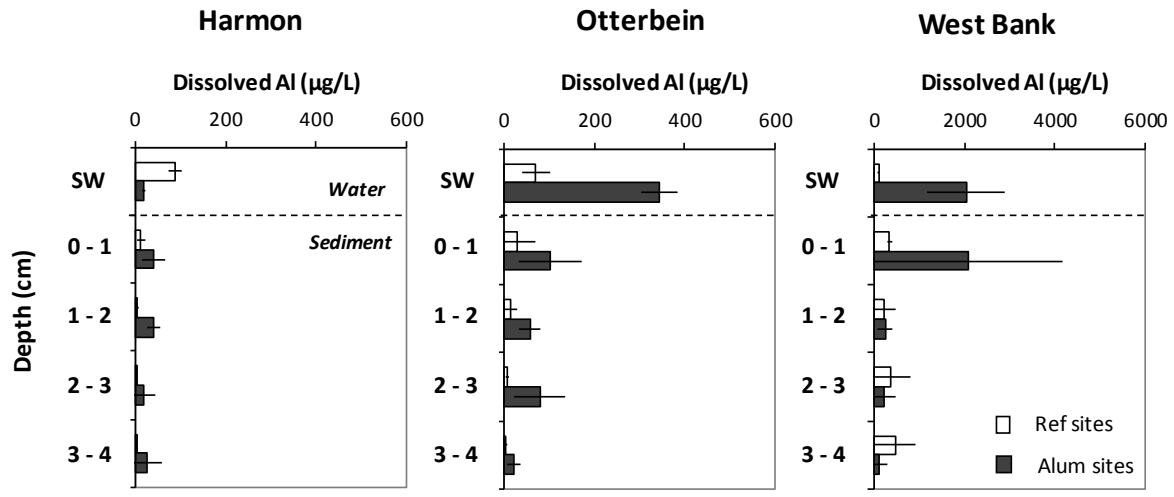

Fig. 5. Aluminum (Al) concentrations in filtered surface and pore waters of the reference (ref) and alum-amended (alum) sites of Harmon, Otterbein and West Bank Marina locations in GLSM (mean ± 1 SE, *n=3*). Note the difference in x-axis scale between the West Bank site and the Otterbein and Harmon sites.

The ecological effects of alum additions are not well known, although this chemical treatment has been used in eutrophic lakes worldwide for four decades (Kennedy and Cooke, 1982). In particular, the effects of alum treatment on benthic microbial and invertebrate communities remain poorly understood. Our results showed decreased total P, TSS, and chlorophyll in the alum test sites (Table 2, Figs. 3 & 4); however, the pH of surface water was increased greatly in each of the alum test sites compared to reference sites (Table 2). While the toxicity of dissolved Al to benthic invertebrates has been well studied under acidic to circumneutral conditions, little information is known about the effects of Al on invertebrates in alkaline water (Gensemer and Playle, 1999). Another consequence of alum additions is an increased amount of sulfate (SO_4^{2-}) in the system. Increased levels of sulfate were measured in the surface water and pore waters of the alum test sites at Harmon and Otterbein (Fig. 6). Sulfate is used as alternative electron acceptor by anaerobic microbial communities and converted into sulfide (S^{2-}), which can be highly toxic to benthic organisms.

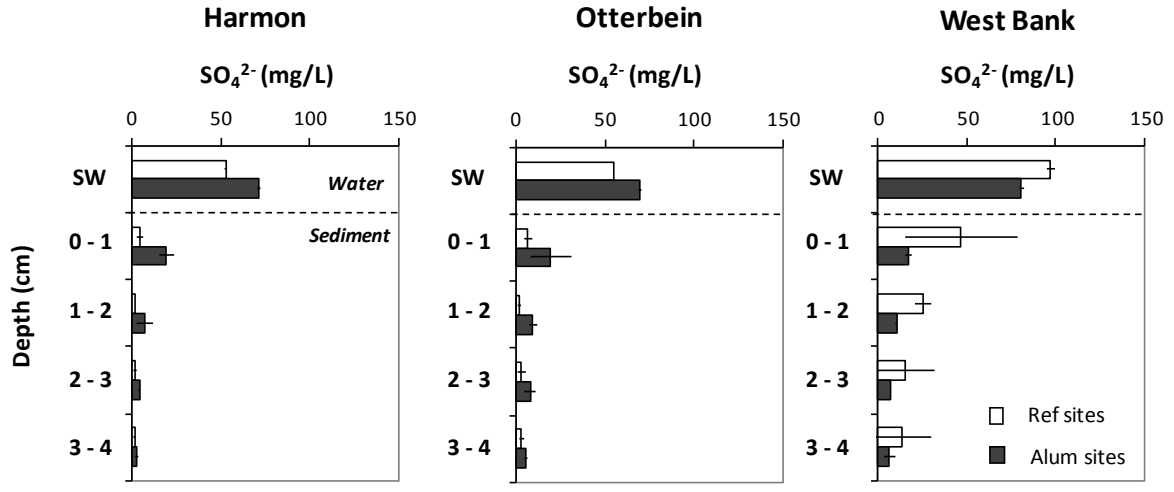

Fig. 6. Concentrations of sulfate (SO_4^{2-}) in the pore water of the reference (ref) and alum test sites of Harmon, Otterbein and West Bank Marina (mean ± 1 SE, *n=3*).

4. Field sampling in Spring/Summer 2011

4.1. Methodology

Our original experimental plan was to sample the untreated reference and alum test sites at each of three locations in the lake in spring and summer 2011. However, in May 2011, the OH EPA decided to treat the *main lake* with alum in order to remove P from the water column and avoid toxic algae bloom during the summer 2011. In June 2011, a high dose of alum was added to 16.2 km^2 (~30% of total lake area) of the central part of GLSM (Figs. 7 and 8). The alum dose was applied from June 2nd to June 29th and corresponded to 390,700 kg Al from alum and 497,265 kg Al from sodium aluminate (OH EPA, 2011).

Fig. 7. Pictures of GLSM and the boat applying alum in June 2011 in the central area of the lake.

In spring and summer 2011, we measured biogeochemical characteristics of water and sediment at five sites of GLSM before (June 2nd 2011) and after (June 29th 2011) the alum addition (Fig. 8). At each site, we measured physicochemical parameters, dissolved ions, TSS, dissolved and particulate metals, and microbial activities in three replicate water samples and sediment cores (Fig. 9). Three replicates of benthic samples also were collected before and after alum addition to measure invertebrate density and species richness.

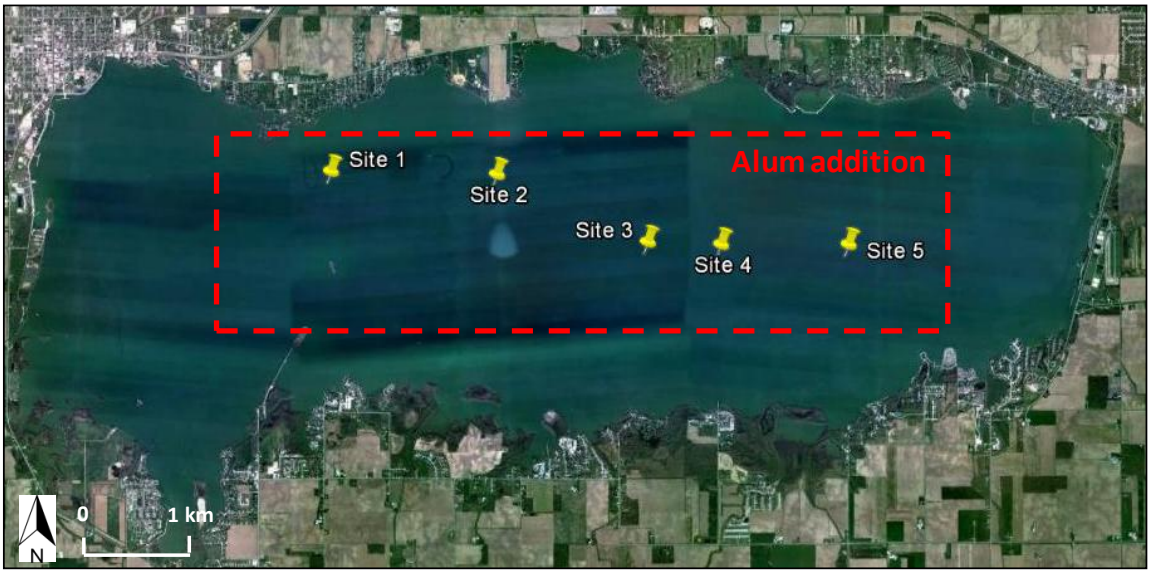

Fig. 8. Map of the sampling sites and area of alum addition applied in June 2011 to the central area of Grand Lake Saint Mary's.

For each field expedition (before and after alum addition), metal analyses were performed on 30 filtered (i.e., 3 replicates, 5 sites, 2 dates) and 30 samples of filtered particles from surface water. We also measured 120 sediment samples (i.e., 3 replicates, 5 sites, 4 depths, 2 dates) and 120 pore water samples resulting in a total of 300 samples for metal analyses. We also measured 90 water samples (i.e., 3 measurements, 3 replicates, 5 sites, 2 dates) for dissolved gases, 30 surface water and 120 pore water samples for nutrients and dissolved organic carbon (DOC), 30 samples for TSS, 240 sediment samples (i.e., 3 replicates, 5 sites, 2 dates, 4 depths, 2 activities) for microbial activity and 30 sediment samples for invertebrate analyses.

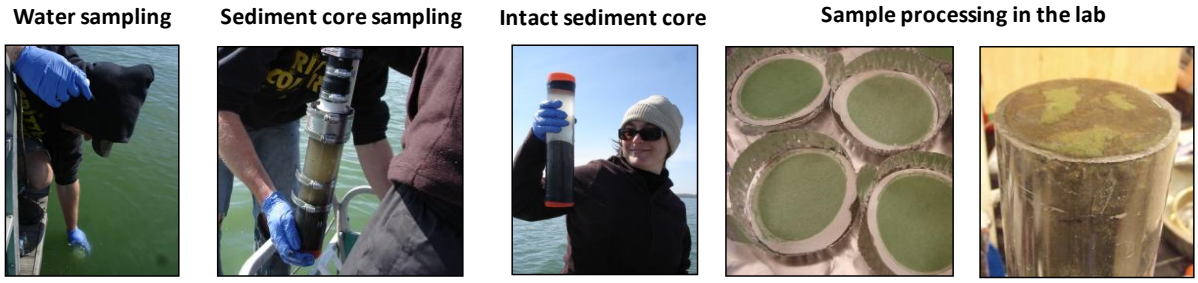

Fig. 9. Pictures of water and sediment sampling and sample processing in the lab in June 2011.

4.2. Principal Findings

The alum addition on the main lake did not affect the chlorophyll concentrations in most of the sampling sites; only a small decrease in chlorophyll was measured at Site 5 after the alum addition in comparison with the pre-alum date (Fig. 10A). The phycocyanin content (i.e., cyanobacteria pigment) of the surface water increased at Sites 1, 2 and 3 of GLSM after the alum addition. These findings suggest that the alum addition did not limit growth of cyanobacteria in the lake, at least within the first week after alum application.

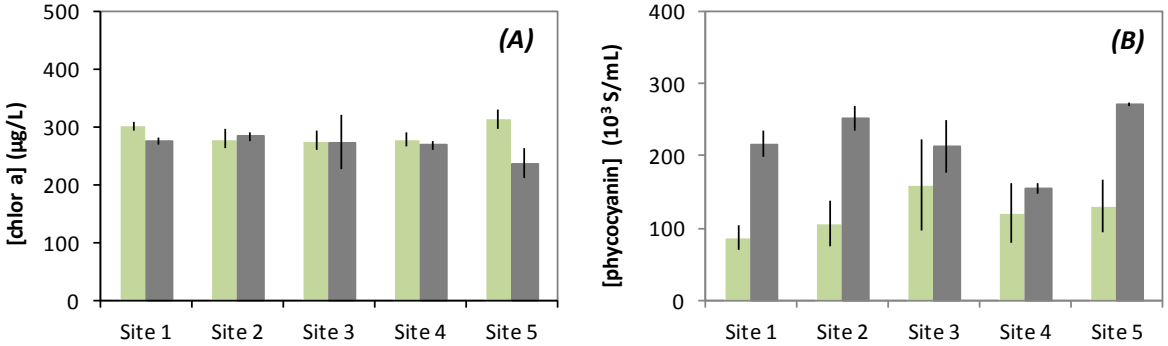

Fig. 10. Concentrations of (A) chlorophyll a and (B) phycocyanin (i.e., cyanobacteria pigment) in the surface water of the five sampling sites of GLSM (i.e., S1 to S5 from the west side to the east side of the lake) before (2nd June 2011) and after (29th June 2011) the alum addition (mean ± 1 SE, *n=3*).

From our pre- and post-alum sampling of lake water, we observed that concentrations of TSS in GLSM were largely unchanged by the addition of alum (Fig. 11A). Compared to pre-alum levels, TSS was increased at Site 1, decreased at Site 5, and unchanged at the other three locations. In contrast, total P concentrations were increased slightly at all sites after the alum addition (Fig. 9B), suggesting that the alum treatment did not significantly remove P from the water column within the first few weeks after application. This is consistent with the observed increase of phycocyanin (i.e., cyanobacterial growth) throughout the month of June (Fig. 10B).

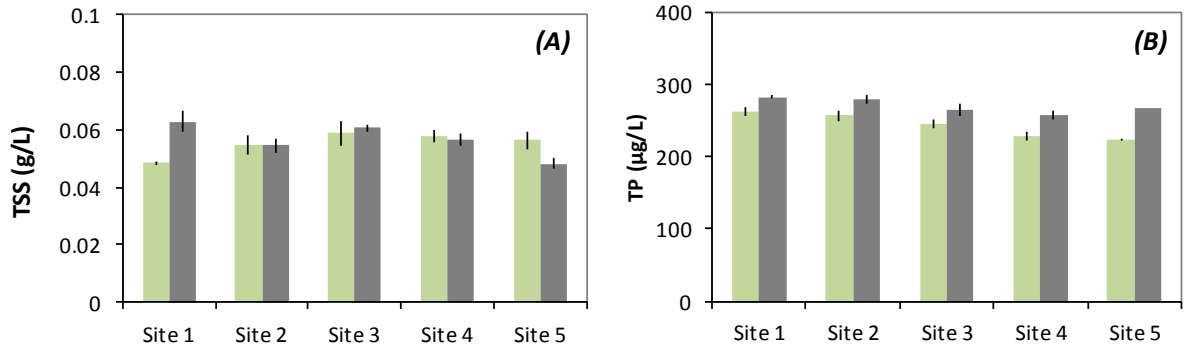

Fig. 11. Concentrations of (A) total suspended solids (TSS) and (B) total phosphorus (TP) in the surface water of the five sampling sites of GLSM before (2nd June 2011) and after (29th June 2011) the alum addition (mean ± 1 SE, *n=3*).

The pH of lake water increased at each of the five sampling sites compared to before the alum addition (Table 3). Such a pH increase is caused by the dissolution of sodium aluminate buffer that is added with the alum. Indeed, levels of Al in filtered surface water after the alum addition (i.e., 614-1650 µg/L) were greatly increased compared to concentrations measured before the alum addition (i.e., 5.8-8.9 µg/L, see on Fig. 12 A). Our first hypothesis that the alum additions would increase Al concentrations in the water and near-surface sediments of GLSM is strongly supported by these results. In a laboratory study, Berkowitz et al. (2005) found that alum addition to water resulted in a rapid initial pH decrease followed by a gradual recovery and an increase of dissolved Al concentrations up to 2500 µg L^{-1} after 17 days and then a decrease to < 250 µg L^{-1} after 150 days. Importantly, and after treatment with alum, there was a 35-d period in Lake Elsinore when aluminum exceeded 1000 µg L^{-1} at a pH of about 8.5 (Berkowitz et al., 2005)—conditions that can cause short-term toxicity (Gensemer and Playle, 1999). We observed similar pH and Al conditions in GLSM (Figs. 5 and 12A for the pilot alum study and the main lake alum addition, respectively). Berkowitz and colleagues (2005) also found that $Al(OH)_3(s)$ formed after alum treatment undergoes geochemical transformations that may decrease its sorption capacity for P and reduce the effectiveness of the alum treatment.

Sulfate concentrations in the surface water did not differ significantly before and after the alum treatment (Fig. 12B), which did not support our second hypothesis stating that alum additions would increase sulfate levels in GLSM. The absence of an increase of sulfate concomitant with Al suggests that sulfate water removed more efficiently from the water column, possibly by either physical (e.g., precipitation) or biological processes (e.g., reduction, uptake).

Table 3. *In-situ* pH measurements in the surface water of the five sampling sites of GLSM before (2nd June 2011) and after (29th June 2011) the alum addition (mean ± 1 SE, *n=3*).

pH surface water	Site 1	Site 2	Site 3	Site 4	Site 5
Before alum	8.6 ± 0.0	8.7 ± 0.0	8.9 ± 0.1	8.8 ± 0.1	8.6 ± 0.0
After alum	9.1 ± 0.4	9.6 ± 0.0	9.5 ± 0.0	9.6 ± 0.0	9.4 ± 0.3

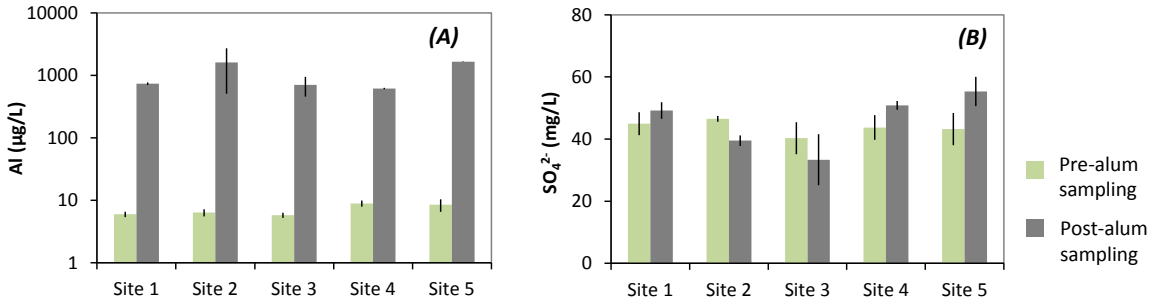

Fig. 12. Concentrations of (A) dissolved sulfate (SO_4^{2-}) and (B) dissolved aluminum (Al) in the surface water of the five sampling sites of GLSM before (2nd June 2011) and after (29th June 2011) the alum addition (mean ± 1 SE, *n=3*). Please note the Al concentration is on a logarithmic scale.

Few studies have focused on the ecological consequences of alum additions on benthic microbial and invertebrate communities. We conducted an invertebrate survey before (i.e., May 5th 2011) and after (July 14th 2011) the addition of alum to GLSM (Fig. 13). Our survey showed that the main taxa found in GLSM sediments were chironomid larvae and oligochaete worms, which are known to be the main taxa tolerant to eutrophic environments. Our results also showed an increase of invertebrate abundances between May and July, which was probably due to a seasonal growth effect and does not allow us to conclude any potential effect of alum on invertebrate abundance. Benthic invertebrate responses to alum addition have contrasting results. Steinman and Ogdadl (2008) observed that alum addition to a lake in Michigan resulted in a substantial reduction of invertebrate density. Moreover, Smeltzer et al. (1999) observed a decrease of invertebrate species density and richness during the first year after alum addition followed by a recovery two years later. In contrast, Narf (1990) observed a general increase of invertebrate density in five Wisconsin lakes after alum treatment. Such contrasted results may depend on the lake nutrient enrichment and geochemistry, the loadings of alum, and the composition of invertebrate communities.

Fig. 13. Pictures of the sediment sampling for the invertebrate survey performed before (5th May 2011) and after (14th July 2011) alum addition

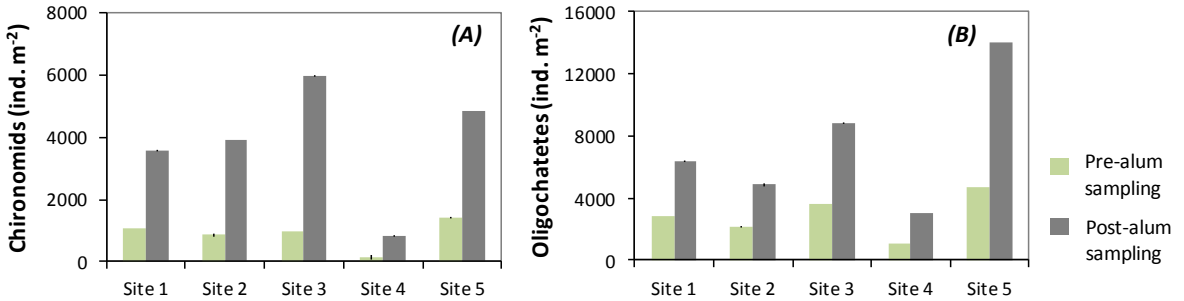

Fig. 14. Chironomid and oligochaetes counts from the invertebrate survey performed before (5th May 2011) and after (14th July 2011) alum addition (mean ± 1 SE, *n=3*)

5. LABORATORY MESOCOSM EXPERIMENT

5.1. Methodology

Our laboratory mesocosm experiment used sediment cores (30 cm height, 7 cm inner diameter) collected from GLSM just prior to the experiment (Fig. 15A). The cores were filled with 10 cm of sediment overlain with 15 cm of water. Sediment was collected from GLSM in June 2011 in a non-alum-amended location and pre-screened with a 1-mm mesh sieve to ensure a relatively homogenous grain size and remove native macrofauna. Experimental cores were filled with aerated surface water from GLSM. With this design we were able to control the addition of alum and the density of macrofauna in order to test the influence and interaction of the two factors on nutrient and metal cycles at the water-sediment interface (Fig. 11B). The experimental cores readily permit (1) periodic sampling of overlying water for metal and chemical analyses, and 2) sectioning of sediment strata at the end of the experiment.

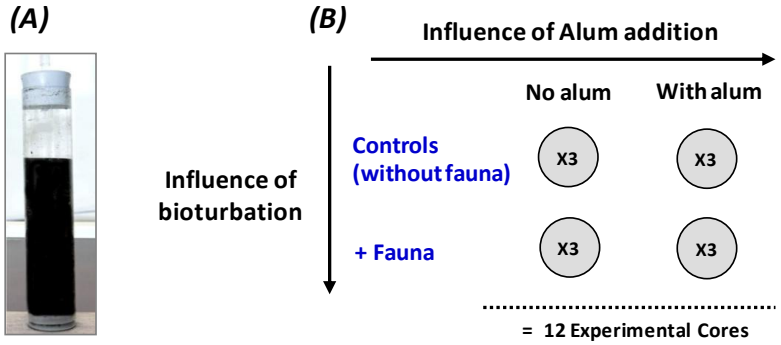

Fig. 15. (A) Picture of one experimental core and (B) design of the mesocosm experiment.

Invertebrates (chironomid larvae) were introduced to the cores after sediment installation. Species identity (i.e., *Chironomus plumosus*) and density (1,200 individuals m^{-2}) of invertebrates for the fauna treatment were determined from the field survey samplings (i.e., Fig. 14A before alum addition). Invertebrates collected from GLSM and were introduced to some of the cores whereas other cores did not have animals and served as controls. Three replicate cores were used for each treatment: (1) no alum, no fauna; (2) no alum, with fauna; (3) with alum, with fauna; and (4) with alum and with fauna (Figs. 15B & 16).

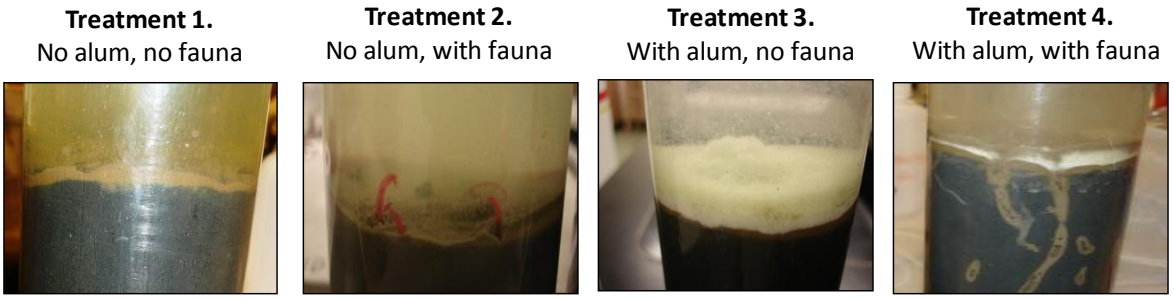

Fig. 16. Picture of different treatments of the experimental cores: (treatment 1) No alum, no fauna; (treatment 2) No alum addition, in presence of chironomid larvae; (treatment 2) with alum addition, absence of chironomid larvae; and (C) with alum addition, in presence of chironomid larvae.

The experiment was initiated by adding alum to the treatment mesocosms three days after the addition of fauna. Liquid alum was added in the designated experimental cores resulting in a total addition of 44 g Al m^{-2}. This loading of alum was selected because it is within the range of those used in pilot tests and other eutrophic lakes (Rydin et al., 2000). During the course of the experiment, water samples (25 mL) were sampled every day in the overlying

water to measure the biogeochemical processes occurring in all sediment cores. This includes measurements of dissolved Al, Mn, Fe, NO_3^-, NO_2^-, NH_4^+, SO_4^{2-}, PO_4^{3-} and total P concentrations before and after animal introduction. At the end of the 7-d incubation, the water layer was removed carefully and sediment was extruded with a piston and sectioned. The majority of the sediment was collected to measure Al, Mn, Fe, P, sulfur, water, and organic matter contents. Pore water was extracted from a subsample of the sediment by centrifugation and 0.45-µm filtration of the supernatant for analysis of metals and nutrients.

5.2. Principal Findings

In the non-alum amended cores, the SRP release from the sediment to the water column increased throughout the 1-week experiment (from day 0 to day 7, see Fig. 17A). The presence of chironomids in the non-alum amended cores induced higher release of SRP early in the test and then a lower release of SRP on days 4 and 7 in comparison to the control cores (no fauna). Such a result can be explained by the bioturbation activities (i.e., burrow building in the sediment) of chironomids in the sediment inducing a stimulation of the nutrient release from the sediment to the water column at the beginning of the experiment. The chironomids also ventilate their burrows to bring O_2 and nutrients in depth (Van de Bund et al., 1994), which could have induced the increase of O_2 concentrations deeper in the sediment and then decreased the release of SRP occurring in the anaerobic layers of the sediment. The addition of alum resulted in a total disappearance of SRP in the surface water of the control cores (Fig. 17B). The presence of chironomids in the alum-amended cores appeared to cause a small release of SRP later in the experiment, suggesting a potential reduction of alum effectiveness in the presence of bioturbating fauna. Our findings are in accordance with Andersen and colleagues (2006), who showed that after the addition of $AlCl_3$ (adjusted to pH 7.5 with 2 M NaOH) to sediment cores, *Chironomus plumosus* larvae created burrows through the Al layer, which caused a significantly increased efflux of P from the Al treated sediment, due to limited contact of P with Al.

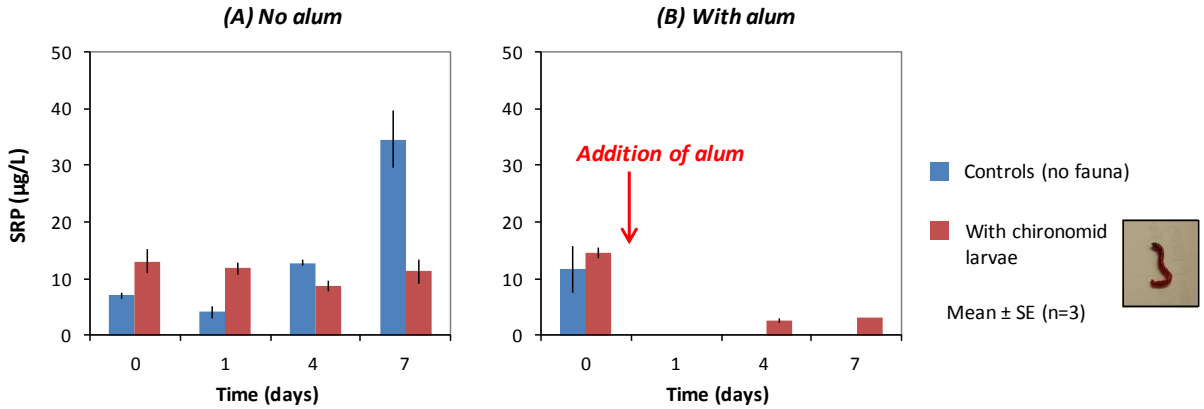

Fig. 17. Concentrations of soluble reactive phosphorus (SRP) in the surface water of the control cores (no fauna) and cores with the presence of chironomid larvae (A) without addition of alum and (B) with addition of alum (mean ± 1 SE, *n=3*).

The concentrations of SRP in the pore water were significantly reduced with the addition of alum in the controls cores (Fig. 18). The presence of chironomid also significantly reduced the SRP concentrations in the pore water in comparison with controls with and without the addition of alum in the experimental cores (Fig. 18). Such results suggest that the ventilation activities of chironomid larvae may have increased the oxygen penetration in the sediment and then reduced the anaerobic release of SRP in the anaerobic sediment layers.

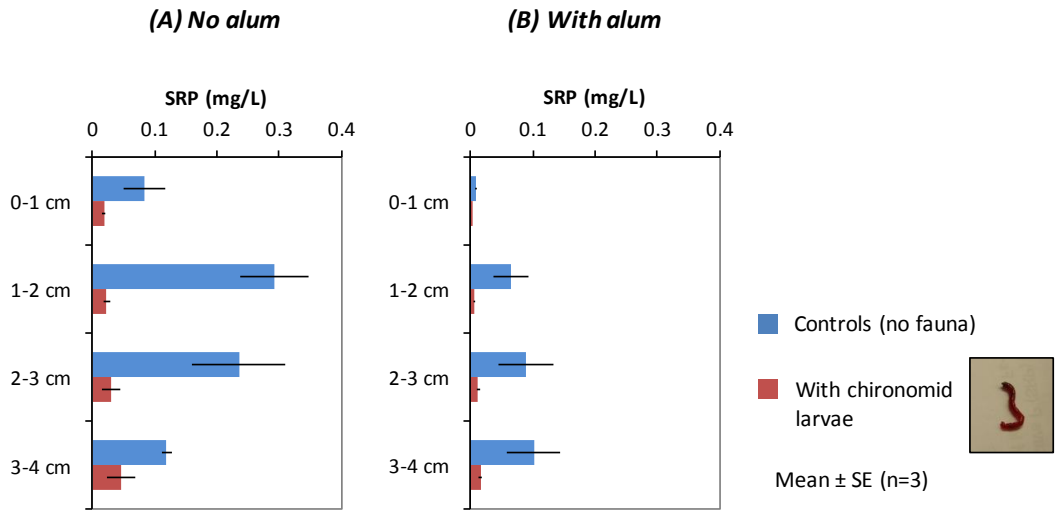

Fig. 18. Concentrations of soluble reactive phosphorus (SRP) in the pore water of the control cores (no fauna) and cores with the presence of chironomid larvae (A) without addition of alum and (B) with addition of alum (mean ± 1 SE, *n=3*).

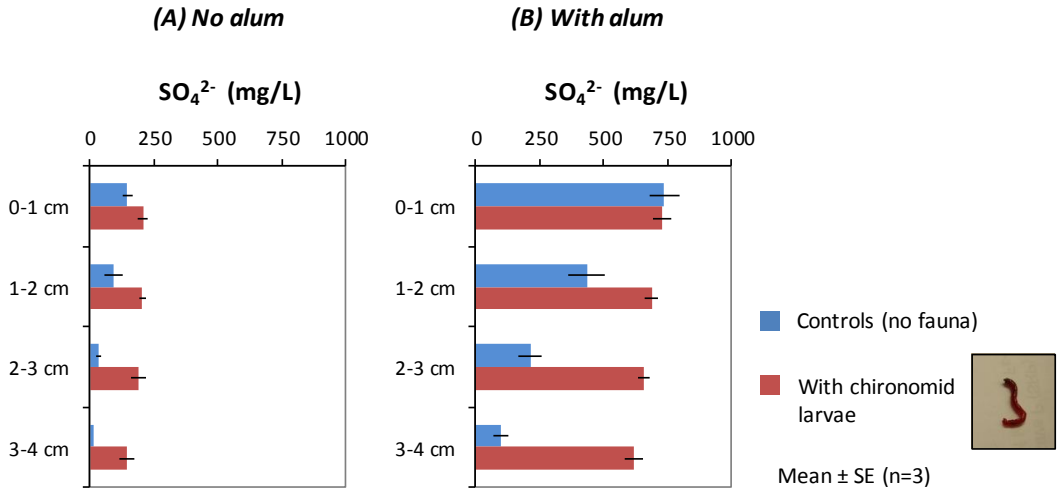

Fig. 19. Concentrations of sulfate (SO_4^{2-}) in the surface water of the control cores (no fauna) and cores with chironomid larvae without addition of alum (A) and with addition of alum (B) (mean ± 1 SE, *n=3*).

The addition of alum greatly increased the concentrations of SO_4^{2-} in pore water (i.e., 150 ± 21 vs. 740 ± 57 mg/L SO_4^{2-} at 0–1 cm depth in the controls without and with addition of alum, respectively, Fig. 19). The concentrations of SO_4^{2-} also decreased with depth in both non-fauna treatments (with and without alum). The results of our mesocosm experiment support our second hypothesis that alum additions would increase sulfate levels in GLSM, which in turn would likely enhanced microbial sulfate reduction rates and generation of sulfide.

The presence of chironomid limited the anaerobic microbial transformation of SO_4^{2-} into toxic S^{2-} at depth with and without alum addition. Such result did not support our third hypothesis that alum additions would decrease invertebrate bioturbation in the sediment, and as a consequence, affect nutrient and metal cycling of GLSM. In contrast, the alum addition did not affect chironomid mortality in the sediment (data not shown) and the effect of chironomid bioturbation probably reduced the potential toxicity of increased sulfate concentrations in the alum-treated sediment.

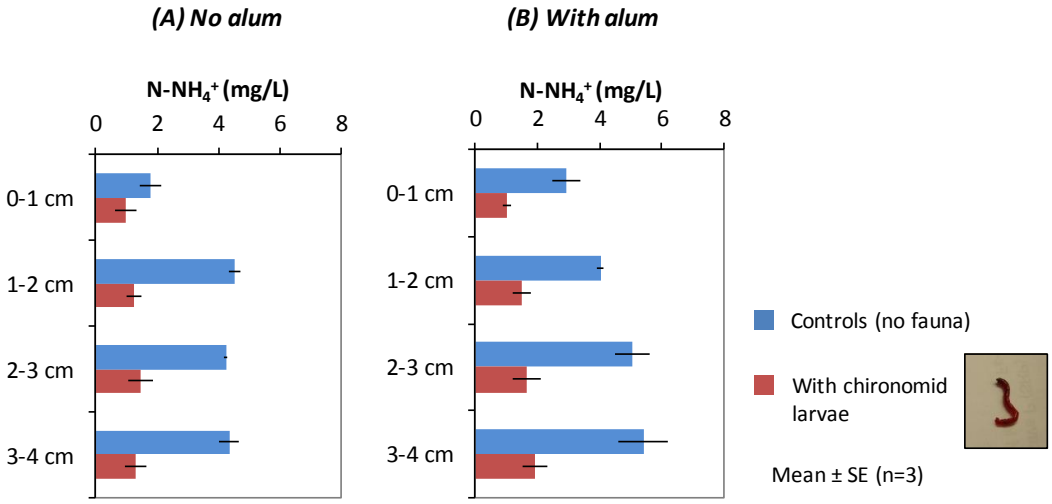

Fig. 20. Ammonium (NH_4^+) concentrations in the pore water of the control cores (no fauna) and cores with the presence of chironomid larvae (A) without addition of alum and (B) with addition of alum (mean ± 1 SE, *n=3*).

As expected, the addition of alum did not affect the NH_4^+ concentrations in the pore water of the control and chironomid cores (Fig. 20). The presence of chironomid greatly decreased the release of NH_4^+ in the sediment, probably due to the increase of O_2 penetration deeper in the sediment in comparison with the controls cores. Our results are in accordance with previous studies showing that chironomid bioturbation can stimulate aerobic microbial community thought their bioturbation activities such as tube building and irrigation (Svensson and Leonardson, 1996; Svensson, 1997; Hansen et al., 1998).

6. SIGNIFICANCE OF THE PROJECT

Because P is often a limiting nutrient in freshwater ecosystems, loadings of P typically increase primary productivity and can lead to eutrophication and water quality degradation. GLSM is a typical example of a recreational lake that has been impacted for years by agriculture (cropland) and livestock operations in its watershed. This has resulted in high P loadings to the lake and subsequent blooms of toxic blue green algae. However, and unfortunately, there is paucity of information on the impacts of P loadings on temporal evolution of GLSM geochemistry and ecology. A recent paper has been published about the impact of agricultural activities on water quality of GLSM and streams in its watershed (Hoorman et al., 2008). This study found that the high P loadings to the lake are a major factor controlling algal blooms and water quality degradation (Hoorman et al., 2008). No data have been published on sediment geochemistry, metal concentrations, benthic communities, or even a simple mass balance for P in GLSM. The results of our study will enhance our knowledge and understanding of the ecological consequences of alum additions in GLSM and, in general, eutrophic freshwater ecosystems. Our findings will provide additional guidance and information to the lake resource managers, consultants and government agencies already working on the environmental issues at GLSM. This research also will provide a framework for other investigations and assessments of Ohio's GLSM restoration and watershed management.

7. PUBLICATIONS AND PRESENTATIONS

7.1. Manuscripts in preparation

Nogaro G., Burgin A.J., Schoepfer V., Konkler M., Bowman K., Hammerschmidt C.R. Alum treatment affects metal and biogeochemical cycling in hypereutrophic lake ecosystem. In preparation for *Journal of Environmental Quality*

Nogaro G., Burgin A.J., Taylor A., Konkler M., Schoepfer V., Hammerschmidt C.R. Can alum prevent harmful algal blooms and restore water quality in Grand Lake St. Mary's, Ohio? In preparation for *Journal of Environmental Quality*

Nogaro G., Burgin A.J., Taylor A., Marsh D., Lam K., Hammerschmidt C.R. Interactions between alum addition and invertebrate bioturbation on nutrient and metal releases in eutrophic lake sediments. In preparation for *Freshwater Biology.*

Taylor, A., Hammerschmidt, C.R., Burgin, A.J., Nogaro, G. Mass balance for phosphorous in eutrophic Grand Lake St. Mary's, Ohio. In preparation for *Water Research.*

7.2. Oral presentations in conferences and seminars

Taylor A., Nogaro G., Burgin, A.J., Hammerschmidt C.R. (2012) Phosphorus budget and benthic flux in eutrophic Grand Lake Saint Mary's, Ohio. Geological Society of America North-Central Section, 46th Annual Meeting, April 23–24 2012, Dayton OH

Nogaro G., Burgin A. J., Hammerschmidt C.R. (2012) Influence of alum addition on metal and nutrient cycling in Grand Lake Saint Mary's, Ohio. Environmental Science Graduate Program's spring seminar series, Ohio State University, April 6 2012, Columbus OH

Nogaro G., Hammerschmidt C.R. Burgin A. J. (2011) Alum influence on metal and nutrient cycling and benthic communities in a shallow eutrophic lake. Annis water Resources Institute seminar series, Grand Valley State University, July 22 2011, Muskegon MI

Nogaro G., Hammerschmidt C.R. Burgin A. J. (2011) Influence of alum addition on metal and nutrient cycling in Grand Lake Saint Mary's, Ohio. North American Benthological Society (NABS) meeting, May 22-26 2011, Providence RI

8. STUDENT SUPPORT

This project provided funding and research opportunities for one undergraduate student (Miss Deepthi Nalluri, biology major) and two graduate students (Ms. Astrea Taylor and Valerie Schoepfer, M.S. Earth & Environmental Sciences) at WSU. These students participated in the field (water and sediment sampling) and laboratory experiments, which afforded them new opportunities for research and professional development. We expect that participation in this collaborative research effort will result in a cohort of broadly-trained, integrative scientists with expertise in geochemistry, microbiology, and ecology.

9. NOTABLE AWARDS AND ACHIEVEMENTS

A Phosphorus Budget for Grand Lake Saint Mary's, Ohio ($9,948) Funded **by the Wright State University Research Council**. C. R. Hammerschmidt (lead), A. J. Burgin, G. Nogaro.

Phosphorus budget and benthic flux in eutrophic Grand Lake Saint Mary's, Ohio ($750) Funded **by Graduate Student Association, Wright State University**. A. Taylor.

10. REFERENCES

Allen N. 2009. Low oxygen causes fish kills. The Daily Standard.

American Public Health Association (APHA), American Water Works Association (AWWA), Water Environment Federation (WEF). 1995. Standard methods for the examination of water and wastewater. 19th ed., Washington, D.C.

Andersen F.Ø., Jørgensen M., and Jensen H.S. 2006. The Influence of *Chironomus plumosus* larvae on nutrient fluxes and phosphorus fractions in aluminum treated lake sediment *Water, Air, Soil Pollut.: Focus* 6: 465-474.

Barlow T. 2010. Killer lake kills property values, tourism jobs. Walletpop. http://www.walletpop.com/blog/2010/08/04/killer-lake-kills-property-values-tourism-jobs/.

Berkowitz J., Anderson M.A., and Graham R.C. 2005. Laboratory investigation of aluminum solubility and solid-phase properties following alum treatment of lake waters. *Water Res. 39: 3918-3928.*

Carpenter S.R., Ludwig D., and Brock. W.A. 1999. Management of eutrophication for lakes subject to potentially irreversible change. *Ecol. Appl.* 9: 751-771.

DeBrossee J. 2010. Grand Lake St. Marys "dying" from toxic algae. Dayton Daily News.

Gensemer R.W. and Playle R. C. 1999. The bioavailability and toxicity of aluminum in aquatic environments. Crit. Rev. *Environ. Sci. Technol.* 29: 315-450.

Gill G.A. and Fitzgerald W.F. 1987. Mercury sampling of open ocean waters at the picomolar level. *Deep-Sea res.* 32: 287–297.

Grieshop S. 2010. Early study: alum won't work. The Daily Standard.

Hammerschmidt C.R., Fitzgerald W.F., Lamborg C.H., Balcom P.H., and Visscher P.T. 2004. Biogeochemistry of methylmercury in sediments of Long Island Sound. *Mar. Chem.* 90: 31–52.

Hansen K., Mouridsen S. and Kristensen E. 1998 The impact of *Chironomus plumosus* larvae on organic matter decay and nutrient (N, P) exchange in a shallow eutrophic lake sediment following a phytoplankton sedimentation. *Hydrobiologia* 364, 65-74.

Hoorman J., Hone T., Sudman T., Dirksen T., Iles J., and Islam K. R. 2008. Agricultural impacts on lake and stream water quality in Grand Lake St. Marys, Western Ohio. *Water, Air, Soil Pollut.* 193: 309-322.

Huang P.M., Wang M.K., Kämpe N., and Schulze D.G. 2002. Aluminum hydroxides. In: Dixon, J.B., Schulze, D.G. (Eds.), Soil Mineralogy with Environmental Applications. SSSA Book Series, No. 7. Soil Sci. Soc. Am., Madison, WI, pp. 261–289.

Kennedy R.H. and Cooke D.G. 1982. Control of lake phosphorus with aluminum sulfate: Dose determination and application techniques. *Water Res. Bull.* 18: 389–395.

Narf R.P. 1990. Interactions of Chironomidae and Chaoboridae (Diptera) with aluminum sulfate treated lake sediments. *Lake Reservoir Manage.* 6: 33–42.

Ohio, State Of. 2010. Grand Lake St. Marys Alum Treatment Pilot Project, no. September.

OH EPA. 2011. Preliminary draft report 2011 Laum treatment and associated water qulity monitoring for Grand Lake St. Marys. Ohio Environmental Protection Agency & Ohio Environmental Protection Agency

Rydin E., Huser B., and Welch E.B. 2000. Amount of phosphorus inactivated by alum treatments in Washington Lakes. *Limnol. Oceanogr.* 45: 226-230.

Sharp J.H., Benner R., Bennett L., Carlson C.A., Fitzwater S.E., Peltzer E.T, and Tupas L.M. 1995. Analyses of dissolved organic carbon in seawater. *Mar. Chem.* 48: 91–108.

Smeltzer E., Kirn R.A., and Fiske S. 1999. Long-term water quality and biological effects of alum treatment of Lake Morey, Vermont. *Lake Reservoir Manage.* 15:173–184.

Smith V.H., Tilman G.D. and Nekola J.C. 1999 Eutrophication: impacts of excess nutrient inputs on freshwater, marine, and terrestrial ecosystems. *Environmental pollution* 100, 179-196.

Steinman A.D. and Ogdahl M. 2008. Ecological effects following an alum treatment in Spring Lake, Michigan. *J. Environ. Qual.* 37: 22-29.

Svensson J.M. (1997) Influence of *Chironomus plumosus* larvae on ammonium flux and denitrification (measured by the acetylene blockage- and the isotope pairing-technique) in eutrophic lake sediment. *Hydrobiologia,* 346, 157-168.

Svensson J.M. and Leonardson L. 1996. Effect of bioturbation by tube-dwelling chironomid larvae on oxygen uptake and denitrification in eutrophic lake sediments. *Freshwat. Biol.* 35, 289-300.

Tetratech. 2010. Recommended actions for Grand Lake St. Marys, Ohio.

Vile M.A., Bridgham S.D., and Wieder R.K. 2003. Response of anaerobic carbon mineralization rates to sulfate amendments in a boreal peatland. *Ecol. Appl.* 13: 720-734.

Wang F.Y. and Chapman P.M. 1999. Biological implications of sulfide in sediment - A review focusing on sediment toxicity. *Environ. Toxicol. Chem.* 18: 2526-2532.

Weston N.B., Dixon R.E., and Joye S.B. 2006. Ramifications of increased salinity in tidal freshwater sediments: Geochemistry and microbial pathways of organic matter mineralization. *J. Geophys. Res.* 111: G01009, doi:01010.01029/02005JG000071.

Generating Renewable Energy on Lake Erie with Wave Energy Converters: A Feasibility Study

Basic Information

Title:	Generating Renewable Energy on Lake Erie with Wave Energy Converters: A Feasibility Study
Project Number:	2011OH239B
Start Date:	3/1/2011
End Date:	2/28/2013
Funding Source:	104B
Congressional District:	15
Research Category:	Engineering
Focus Category:	Models, Water Supply, Conservation
Descriptors:	
Principal Investigators:	Ethan John Kubatko

Publications

1. Dibling, Dave; Ethan Kubatko, Generating Renewable Energy on Lake Erie with wave energy converters: a feasibility study, Great Lakes Research, in preparation.
2. Kubatko, Ethan, 2011, Development of a high-resolution, nearshore model for Lake Erie, The 10th International Workshop on Multiscale (Un-)structured Mesh Numerical Modelling for coastal, shelf and global ocean dynamics, August 2011.
3. Kubatko, Ethan, 2012, Validation of a high-resolution finite element model for Lake Erie, In World Congress on Computational Mechanics, July 2012.

GENERATING RENEWABLE ENERGY ON LAKE ERIE WITH WAVE ENERGY CONVERTERS: A FEASIBILITY STUDY

Principal Investigator:

Ethan J. Kubatko, Assistant Professor
Department of Civil & Environmental Engineering & Geodetic Science
The Ohio State University

1 Research Objectives

The primary objective of this research is to investigate the feasibility of generating clean, renewable energy on Lake Erie by harnessing the Lake's wave energy through the use of a novel kinetic energy harvesting technology called nPower® developed by Tremont Electric, LLC, a Cleveland-based alternative energy company. Specifically, feasibility of this idea will be investigated by performing wave energy simulations that make use of two critical modeling components described in detail below: 1) a *high-resolution*, *unstructured mesh* of Lake Erie that provides highly accurate measurements of the bathymetry and the shoreline of the Lake, see Figure 4; and 2) a *computational model* that consists of a tightly coupled two-dimensional shallow water circulation/spectral wave energy evolution model.

2 Methodology

The current hydrodynamic model used by the Lake Erie Operational Forecast System or LEOFS is the Princeton Oceanic Model or POM. The POM model was developed primarily by Dr. Alan Blumberg and Dr. George Mellor in the late 1970's and uses and sigma coordinate (vertical), curvilinear coordinate (horizontal), free surface, ocean model that also uses a turbulent sub-model. The current POM version used by GLOFS has been modified by Dr. David Schwab of NOAA's Great Lakes Environmental Research Laboratory (GLERL) and by researchers from The Ohio State University. As its input, The model takes surface meteorological data, such as surface wind speed and air temperature, which are obtained from, for example, U.S. and Canadian meteorological buoys (nowcast mode) and the National Weather Services operational North American Mesoscale (NAM) weather forecast model (forecast mode). However, the current models inability to accurately model the nearshore region of Lake Erie has induced the idea that a new model may need to be used to capture this region of Lake Erie.

Besides POM, other potential hydrodynamic models include ADCIRC, GEMSS, QUODDY, ROMS, and DYNLET. However, the flexibility of ADCIRC to be coupled with a wave model(SWAN) makes it the easiest to use. It has been tested and validated in a variety of

different applications such as modeling tides & wind driven circulation, analysis of hurricane storm surge & flooding, dredging feasibility & material disposal studies, larval transport studies, and nearshore marine operations. The ability of ADCIRC to model wind driven circulation in the nearshore region makes it a reputable choice for usage on Lake Erie because Lake Erie is driven by wind .

2.1 Governing Equations

The three main equations that govern the ADCIRC model are the shallow water equations which are the depth-averaged continuity equation($\mathcal{L}$) and the 2D momentum equation($\mathcal{M}$). These hyperbolic PDEs are derived from the Navier-Stokes equations which are the general equations for fluid motion and are:

$$\mathcal{L} \equiv \frac{\partial \zeta}{\partial t} + \nabla \cdot \mathbf{q} = 0 \tag{1}$$

$$\mathcal{M} \equiv \frac{\partial \mathbf{q}}{\partial t} + \nabla \cdot \left(\mathbf{q}\mathbf{q}/H\right) + \tau_{bf}\mathbf{q} + \mathbf{f}_c \times \mathbf{q} + gH\nabla\zeta - \varepsilon\Delta\mathbf{q} - \mathbf{F} = \mathbf{0} \tag{2}$$

The equations above are able to solve the 3 unknowns ζ, u and v. From Equation 1, ζ is the height or elevation of the free surface and $\mathbf{q} \equiv (Hu, Hv)$,where the total height of the water column, $\zeta + h_b$, is H and where u and v are the depth-integrated horizontal velocities or currents. The distance from the datum to the bottom or bathymetric depth(positive downward) is h_b. The constant surface elevation or datum in the case of Lake Erie is set at 184 meters above sea level. The reference datums for bodies of water are generally taken when the water is still. From Equation 2, the bottom friction factor is τ_{bf}, the Coriolis force is $\mathbf{f}_c$, acceleration due to gravity is g, the eddy viscosity coefficient is ε, and $\mathbf{F}$ can potentially, depending on the inputs, contain multiple stresses and forces such as wave radiation stresses, wind radiation stresses, variable atmospheric pressure, and tidal potential forces.

2.2 ADCIRC

The *ADvanced CIRCulation model for oceanic, coastal and estuarine water* or ADCIRC was created as a means of solving 2D and 3D time dependent, free surface circulation and transport problems. ADCIRC offers the user the ability to run in serial or in parallel which allows for faster simulation run times. It also uses the continuous Galerkin method in solving the finite element mesh.

ADCIRC uses the 2D Momentum Equations as they appear in Equations 2; however, they make various manipulations of the Continuity Equation in 1 to create the Generalized Wave Continuity Equation or GWCE, and can be written as:

$$\frac{\partial \mathcal{L}}{\partial t} + \nabla \cdot \mathcal{M} + \tau_0 \mathcal{L} = 0 \tag{3}$$

The GWCE is a weak weighted residual that is solved by ADCIRC along with the 2D momentum equation. During the manipulations of these equations, a user-defined weighting

factor,τ_0, is created. This weighting factor weights the relative contribution of the primitive wave portions of the GWCE. τ_0 is basically a factor that needs to be adjusted and fine tuned to disperse the solution enough as to not cause oscillatory solutions in your model so it runs smoothly. The τ_0 variable is something that only exists in the continuous Galerkin method, CG, version of ADCIRC and not the discontinuous Galerkin method, DG, version of ADCIRC.

Carrying out the partial time derivative of $\mathcal{L}$ and and the $\nabla \cdot \mathcal{M}$ from Equation 3, the GWCE is expanded into:

$$\frac{\partial^2 \zeta}{\partial t^2} + \tau_0 \frac{\partial \zeta}{\partial t} + \frac{\partial J_x}{\partial x} + \frac{\partial J_y}{\partial y} - uH\frac{\partial \tau_0}{\partial x} - vH\frac{\partial \tau_0}{\partial y} = 0, \tag{4}$$

where:

$$\begin{aligned} J_x = -uH\frac{\partial u}{\partial x} - vH\frac{\partial u}{\partial y} + \mathbf{f}_c vH - \frac{g}{2}\frac{\partial \zeta^2}{\partial x} - gH\frac{\partial}{\partial x}\left(\frac{P_{H_20}}{g\rho_0} - \alpha\eta\right) \\ + \frac{\tau_{sx,winds} + \tau_{sx,waves} - \tau_{bx}}{\rho_0} + (M_x - D_x) + u\frac{\partial \zeta}{\partial t} + \tau_0 uH - gH\frac{\partial \zeta}{\partial x}, \end{aligned} \tag{5}$$

$$\begin{aligned} J_y = -uH\frac{\partial v}{\partial x} - vH\frac{\partial v}{\partial y} + \mathbf{f}_c uH - \frac{g}{2}\frac{\partial \zeta^2}{\partial y} - gH\frac{\partial}{\partial y}\left(\frac{P_{H_20}}{g\rho_0} - \alpha\eta\right) \\ + \frac{\tau_{sy,winds} + \tau_{sy,waves} - \tau_{by}}{\rho_0} + (M_y - D_y) + v\frac{\partial \zeta}{\partial t} + \tau_0 vH - gH\frac{\partial \zeta}{\partial y}, \end{aligned} \tag{6}$$

and the vertically-integrated momentum equations determine the currents by:

$$\begin{aligned} \frac{\partial u}{\partial t} + u\frac{\partial u}{\partial x} + v\frac{\partial u}{\partial y} - \mathbf{f}_c v = -g\frac{\partial}{\partial x}\left(\zeta + \frac{P_{H_20}}{g\rho_0} - \alpha\eta\right) + \\ + \frac{\tau_{sx,winds} + \tau_{sx,waves} - \tau_{bx}}{\rho_0 H} + \left(\frac{M_x - D_x}{H}\right), \end{aligned} \tag{7}$$

and:

$$\begin{aligned} \frac{\partial v}{\partial t} + u\frac{\partial v}{\partial x} + v\frac{\partial v}{\partial y} - \mathbf{f}_c u = -g\frac{\partial}{\partial y}\left(\zeta + \frac{P_{H_20}}{g\rho_0} - \alpha\eta\right) + \\ + \frac{\tau_{sy,winds} + \tau_{sy,waves} - \tau_{by}}{\rho_0 H} + \left(\frac{M_y - D_y}{H}\right), \end{aligned} \tag{8}$$

where the atmospheric pressure at the water surface is P_{H_20}, the reference density of water is ρ_0, the Newtonian equilibrium tidal potential is η, and the effective earth elasticity factor is α; the surface stresses caused by winds and waves are $\tau_{sx,winds}$, $\tau_{sy,winds}$, $\tau_{sx,waves}$, and $\tau_{sy,waves}$; the bottom stresses are τ_{bx} and τ_{by}; the lateral stress gradients are M_x and M_y, and the momentum dispersion terms are D_x and D_y. The unknown water level(ζ) and currents (u and v) can be computed by ADCIRC using a linear Lagrange interpolation and solving these expanded Equations 4, 7, and 8 for the three degrees of freedom at every node of the finite element mesh.

2.2.1 ADCIRC Inputs

There are 5 input files that are read by ADCIRC in which 2 of them are required and the other 3 are conditional depending on what your simulation needs are. The *Grid and Boundary Information File* or fort.14 is required and is the the actual finite element mesh that you wish to use. The finite element mesh and the boundary conditions types need to be established in this file. The *Model Parameter and Periodic Boundary Condition File* or fort.15 is the other required input file. The fort.15 file contains most of the parameters required to run ADCIRC. Some of these parameters include the timestep interval, run duration, ramping function options, the τ_0 value you wish to use, meteorological wind/pressure interval, normal flow boundary flow rates, and the station's longitude & latitude for which you would like to have data written for and the interval at which the data should be written. The *Single File Meteorological Forcing Input* or fort.22 is used to inform ADCRIC the number the meteorological fields to be used, the offset that the meteorological data starts in comparison to the start time of the ADCIRC run(if there is one), and the wind velocity multiplication factor. The *Multiple File Meteorological Forcing Input* or fort.221 & fort.222 are the methods used to force the Lake Erie model other than river flows. The fort.221 contains atmospheric pressure recorded by stations around Lake Erie and are measured in units of Pascals(millibars). The fort.222 contains wind velocity in the u and v components from recording stations around Lake Erie at 10 meter heights above the water surface and are in units of m/s.

Once the pressure and wind velocities are read into ADCIRC, the following relationships are computed;

$$P_{H_20} = \frac{P}{100 \times g \times \ \gamma_{H_20}} \tag{9}$$

$$W_S = \|W_V\| \tag{10}$$

$$D_C \ = \ 0.001 \times (0.75 \ + \ 0.067 \times W_S) \tag{11}$$

$$W_{ST} \ = \ D_C \times 0.001293 \times W_V \times W_S \tag{12}$$

where P is the atmospheric pressure read from the fort.221, γ_{H_20} is the density of water, W_S is the wind speed, W_V is the wind velocity read from the fort.222, D_C is the drag coefficient, and W_{ST} is the wind stress. If the calculated D_C is greater than 0.003, then the D_C is set to 0.003.

2.2.2 ADCIRC Outputs

ADCIRC has multiple outputs from which we can use to verify against recorded data at specified meteorological that the model is working; such as, the elevation time series or surface elevation (fort.61), the atmospheric pressure time series(fort.71), and the wind velocity time series(fort.72). The elevation time series is the most important output from ADCIRC, because unlike the atmospheric pressure and wind velocity, the change in the water surface elevation is not an input into ADCIRC. Because of this, matching the recorded surface elevation to the ADCIRC results goes a long way into verifying the model. The depth-averaged

velocity time series(fort.62) cannot be compared with recorded data because there are no recordings for depth averaged velocity in Lake Erie; however, it can be used to compare the differences in the depth-averaged velocity the ADCRIC+SWAN results.

Another way of validating the model is comparing the significant wave heights recorded at the 3 meteorological buoys that are all located in the open water. However ADCIRC only solves the modified forms of the Shallow Water Equations so it is unable to determine the significant wave heights. This is why the SWAN model, one that can model the wave heights, is coupled with ADCIRC so this validation is possible.

2.3 ADCIRC + SWAN

Simulating WAves Nearshore or SWAN was developed to determine wave propagation in time and space, shoaling, refraction due to current and depth, frequency shifting due to currents and non-stationary depth. For our model, the most important physics that SWAN accounts for is the wave generation by wind because as mentioned before, Lake Erie is primarily a wind driven lake. Other physics that SWAN accounts for are white capping, depth-induced breaking, dissipation due to vegetation, and diffraction. The SWAN equation, $\mathcal{S}$, accounts for the wave action density $N(\lambda, \varphi, \sigma, \theta, t)$ as it moves through geographic space (λ, φ) and spectral space (with relative frequencies σ and direction θ), in time (t),the action balance equation is governed by:

$$\begin{aligned} \mathcal{S} \equiv \frac{\partial N}{\partial t} \; + \; \frac{\partial}{\partial \lambda}\left[\left(c_\lambda + u\right) N\right] \; + \; \arccos\varphi \frac{\partial}{\partial \varphi}\left[\left(c_\varphi + v\right) N \cos\varphi\right] \\ + \; \frac{\partial}{\partial \theta}\left[c_\theta N\right] \; + \; \frac{\partial}{\partial \sigma}\left[c_\sigma N\right] \; = \; \frac{S_{tot}}{\sigma} \end{aligned} \tag{13}$$

where (u, v) are the ambient current, (c_λ, c_φ) are the group velocities, c_θ is the propagation velocity in the θ-space, and c_σ is the propagation velocity in the σ-space. S_{tot} is the source term that represents how the wind determines the growth of the waves by:

- surf breaking and bottom friction,
- action lost due to whitecapping,
- and action in deep water and shallow water of the exchange between spectral components caused by nonlinear effects.

SWAN communicates with ADCIRC in order to obtain the necessary wind speeds, water levels, and currents that ADCIRC calculates at each node. These three components are essentially what drives the SWAN model. For a given timestep, these components are first calculated by ADCIRC, then they are passed onto SWAN where it recalculates the water level and all related wave processes. These SWAN values are then read back into ADCIRC at each node where the process repeats itself for the next timestep. When running ADCIRC+SWAN, only one of the models can run at once because each model needs information from the other in order to force it. The radiation stress gradients, $\tau_{sx,waves}$ & $\tau_{sy,waves}$, partially drive and force ADCIRC and are computed by SWAN by the following equations;

$$\tau_{sx,waves} \; = \; -\frac{\partial S_{xx}}{\partial x} \; - \; \frac{\partial S_{xy}}{\partial y}, \tag{14}$$

$$\tau_{sy,waves} = -\frac{\partial S_{xy}}{\partial x} - \frac{\partial S_{yy}}{\partial y}, \tag{15}$$

where the wave radiation stresses are S_{xx}, S_{xy} and S_{yy}. The radiation stresses, which are constant on each element, are interpolated into the space of continuous, piecewise linear functions and differentiated to obtain the radiation stress gradients in Equations 14 & 15. The wave radiation stresses are computed at the mesh node and are defined as;

$$S_{xx} = \rho_0 g \int\int \left(\left(n\ cos^2\theta + n - \frac{1}{2}\right)\sigma N\right) d\sigma d\theta, \tag{16}$$

$$S_{xy} = \rho_0 g \int\int \left(n\ sin\theta\ cos\theta\ \sigma N\right) d\sigma d\theta, \tag{17}$$

$$S_{yy} = \rho_0 g \int\int \left(\left(n\ sin^2\theta + n - \frac{1}{2}\right)\sigma N\right) d\sigma d\theta, \tag{18}$$

where n is the ratio of group velocity to phase velocity. Equations 16 – 18 are computed before Equations 14 & 15. An area-weighted average of the gradients is used to project the element-based gradients to the elements adjacent to each mesh node.

There are many outputs from SWAN which include average wave direction, directional spreading, wave energy, and dissipation but the most useful output is the significant wave height. This value can be compared to the recorded results from the 3 Lake Erie buoys, thus adding another comparison to help validate the model. Once validation has occurred, the wave energy can be used to determine locations for the wave energy converters.

3 Principal Findings & Significance

The mesh on which ADCIRC+SWAN runs on was created using up-to-date shoreline that was traced and the newest bathymetry data. The resulting mesh contains 401,547 nodes connecting 782,650 elements and can be seen in Figure 1. The size of individual elements ranges from 10 meter in rivers/channels/marinas to 3 kilometers in the open water where there is little to no change in bathymetry.

Monthly simulations were run from May through October because these are the months that have the weather buoy data available to compare the model simulations to. The years that the simulations were run for were 2009, 2010, and 2011. A comparison of the weather buoys 45005, 45132, and 45142 to the ADCIRC+SWAN output for both May 2009 and August 2009 is shown in Figures 2 - 7. The gaps in the Recorded Data(blue line) indicate times in which the station was not recording. Overall the model has shown it's ability to capture the peaks and general trends of the recorded data.

The maximum monthly waves heights for May 2009 and August 2009 are shown in figures 8 & 9. Computing the max height values for the entire lake at every node provides us with information on where the max elevation is most likely to occur and therefor be the best place to implement the wave energy converters.

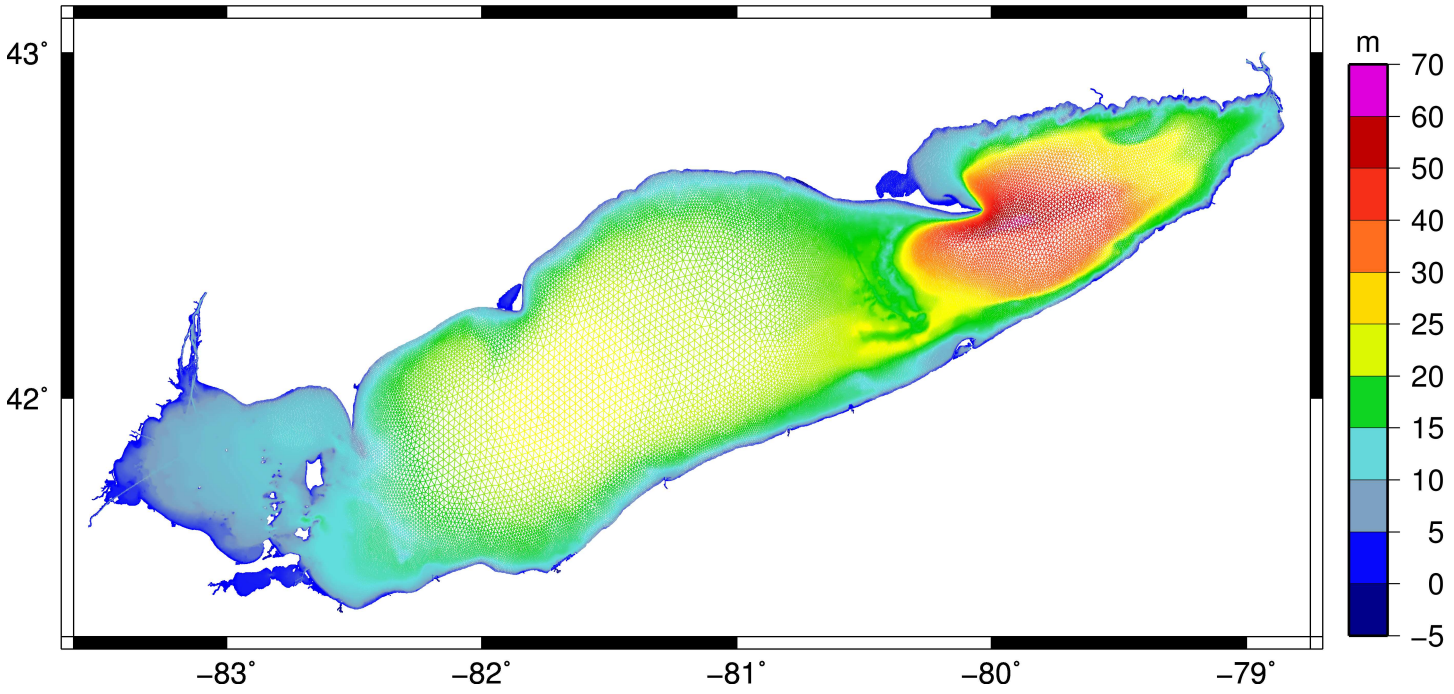

Figure 1: Lake Erie Mesh with Bathymetry

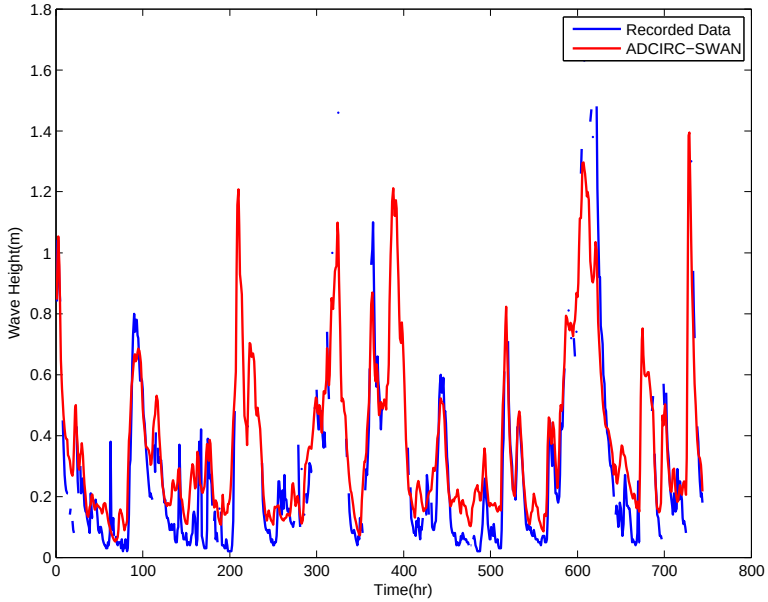

Figure 2: May 2009 Significant Wave Height at Buoy 45005

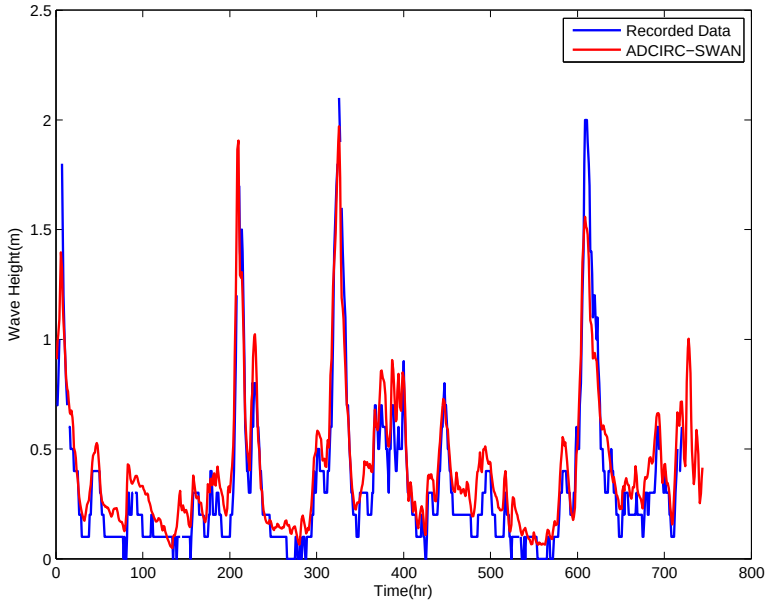

Figure 3: May 2009 Significant Wave Height at Buoy 45132

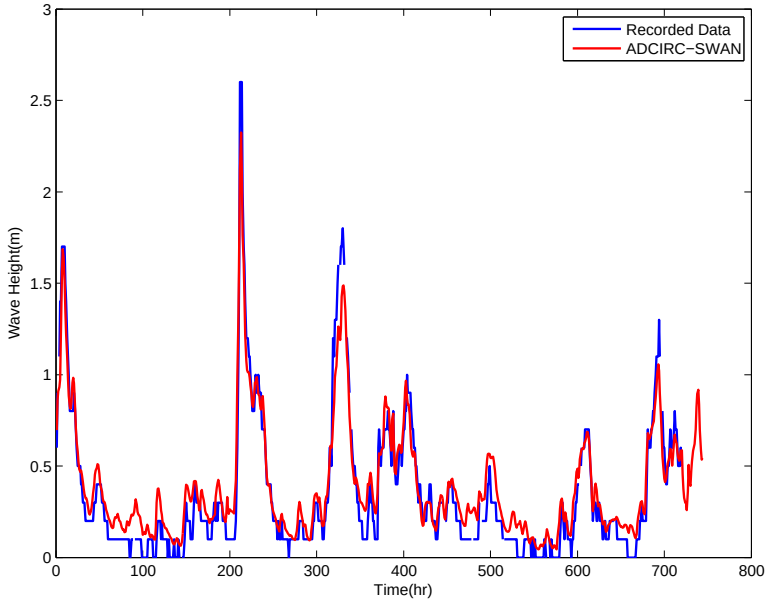

Figure 4: May 2009 Significant Wave Height at Buoy 45142

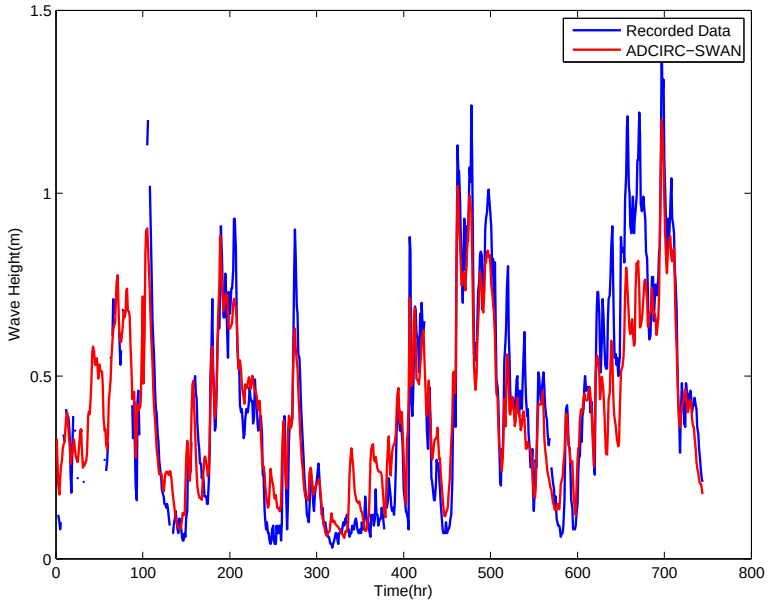

Figure 5: August 2009 Significant Wave Height at Buoy 45005

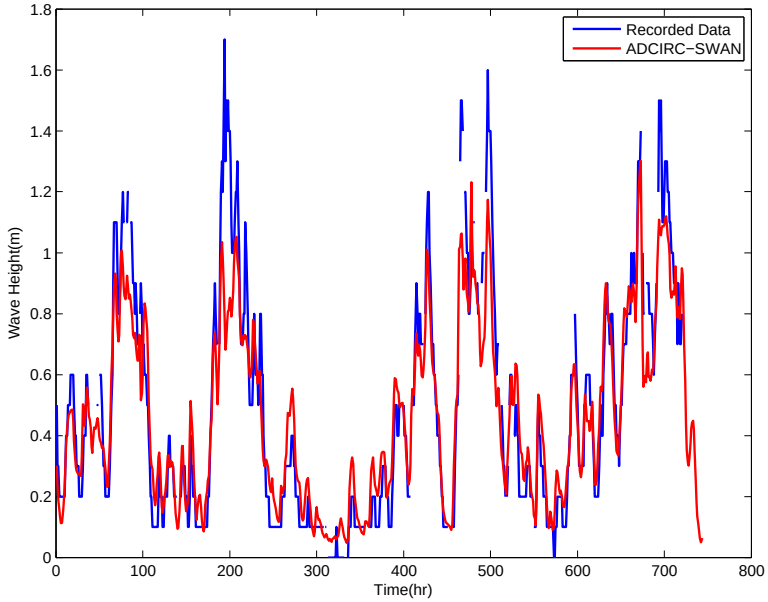

Figure 6: August 2009 Significant Wave Height at Buoy 45132

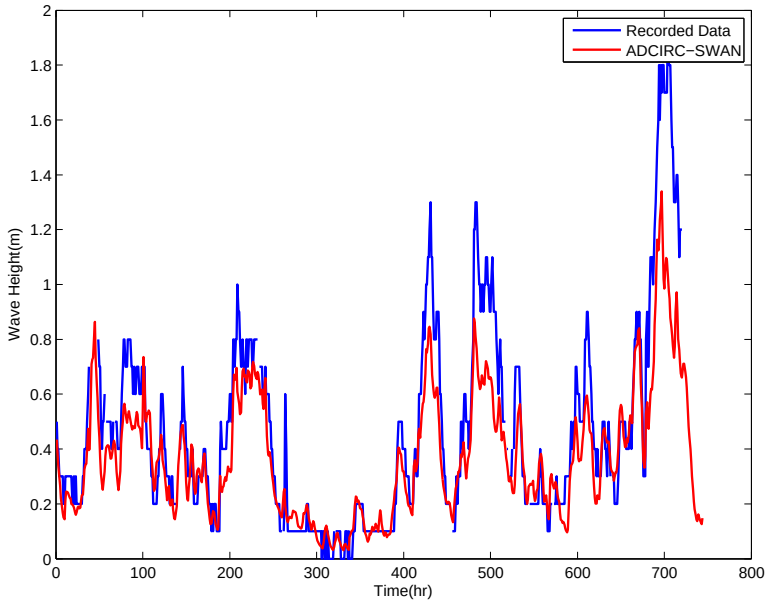

Figure 7: August 2009 Significant Wave Height at Buoy 45142

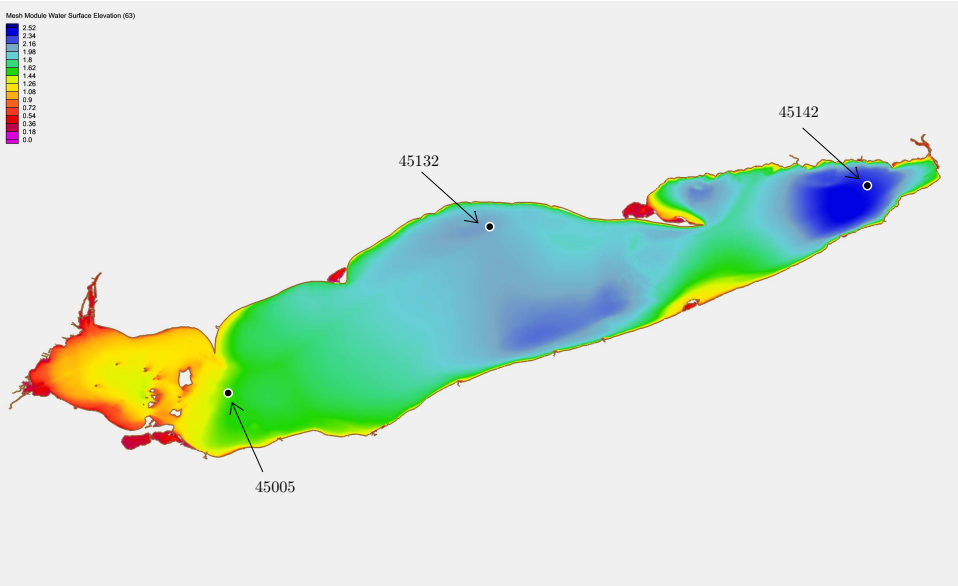

Figure 8: May 2009 Maximum Wave Heights

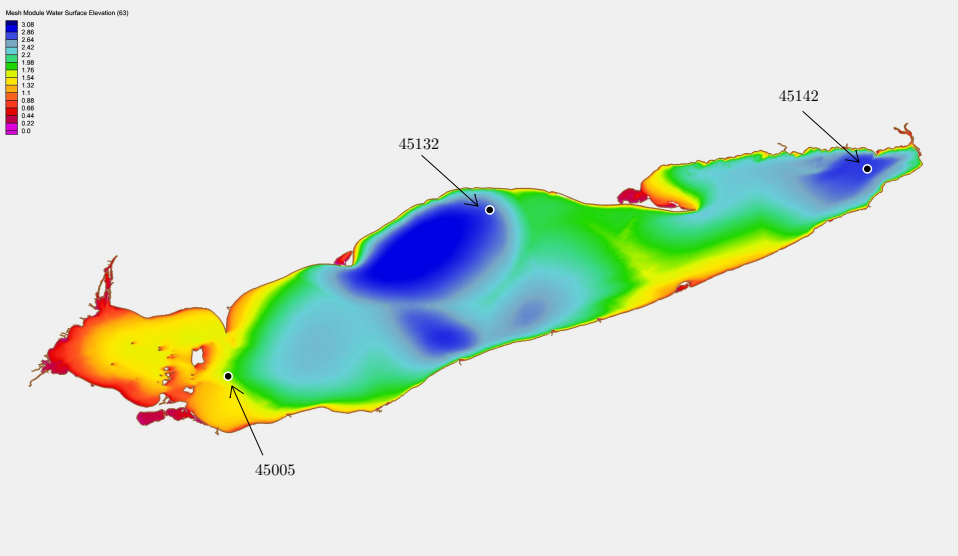

Figure 9: August 2009 Maximum Wave Heights

High-performance Porous Polybenzimidizole Membranes For Water Treatment Using Forward Osmosis

Basic Information

Title:	High-performance Porous Polybenzimidizole Membranes For Water Treatment Using Forward Osmosis
Project Number:	2011OH290O
Start Date:	5/1/2011
End Date:	2/28/2013
Funding Source:	Other
Congressional District:	9
Research Category:	Engineering
Focus Category:	Treatment, Methods, Water Quality
Descriptors:	
Principal Investigators:	Isabel Escobar

Publications

1. Flanagan Michael; Isabel Escobar, submitted 2012, Novel Charged and Hydrophilized Polybenzimidazole (PBI)Membranes for Forward Osmosis,Journal of Membrane Science.
2. Flanagan Michael; Richard Hausman, Brett Digman, Isabel Escobar, Maria Coleman, TS Chung, 2011, Surface Functionalization of Polybenzimidazole Membranes to Increase Hydrophilicity and Charge.In:Escobar I.C.and B. Van der Bruggen (eds.), Modern Applications in Membrane Science and Technology. ACS Symposium Series; American Chemical Society: Washington, DC, pages 303-– 322.
3. Flanagan Michael; Richard Hausman, Isabel Escobar, Maria Coleman, TS Chung, 2012, Functionalization of Polybenzimidazole Membranes for Pore Size Reduction, Increased Hydrophilicity and Surface Charge, In 2012 AIChE Spring Meeting, Houston, TX, April 1-–5.
4. Flanagan Michael; Richard Hausman, Isabel Escobar, 2011, Polybenzimidazole Forward Osmosis Membranes Functionalized to Impart Surface Charge and An Increase In Hydrophilicity, In 2011 AIChE Annual Meeting, Minneapolis, MN, October 16-–21, 2011.
5. Flanagan Michael; Richard Hausman, Isabel Escobar, Maria Coleman, TS Chung, 2011, Polybenzimidazole Forward Osmosis Membranes Functionalized for Increased Surface Charge and Hydrophilicity, In 2011 NAMS Annual Meeting, Las Vegas, NV, June 4-–8.

High-performance porous polybenzimidizole membranes for water treatment using forward osmosis

Progress Report

The University of Toledo PI: Isabel C. Escobar, Chemical and Environmental Engineering, The University of Toledo, MS 305, Toledo, OH 43606-3390, USA Tel: +1-419-530-8267, Fax: +1-419-530-8086, Email:Isabel.Escobar@utoledo.edu

Students Supported: (1) Michael F. Flanagan, MS in Chemical Engineering; and (2) Jordan Morales, undergraduate, BS in Chemical and Environmental Engineering

Publications:

1. Flanagan M., and I.C. Escobar (submitted, 2012). Novel Charged and Hydrophilized Polybenzimidazole (PBI) Membranes for Forward Osmosis, *Journal of Membrane Science.*
2. Flanagan, M., Hausman, R., Digman B., I.C. Escobar, M.R. Coleman, and T-S Chung (2011). Surface Functionalization of Polybenzimidazole Membranes to Increase Hydrophilicity and Charge. In: Escobar I.C. and B. Van der Bruggen (eds.), Modern Applications in Membrane Science and Technology. ACS Symposium Series; American Chemical Society: Washington, DC, pages 303-322.

Presentations:

1. Flanagan M., R. Hausman, and I.C. Escobar, M. Coleman, and T-S Chung (2012). "Functionalization of Polybenzimidazole Membranes for Pore Size Reduction, Increased Hydrophilicity and Surface Charge," 2012 AIChE Spring Meeting, Houston, TX, April 1-5, 2012.
2. Flanagan M., R. Hausman, and I.C. Escobar (2011). "Polybenzimidazole Forward Osmosis Membranes Functionalized to Impart Surface Charge and An Increase In Hydrophilicity," 2011 AIChE Annual Meeting, Minneapolis, MN, October 16-21, 2011.
3. Flanagan M., R. Hausman, I.C. Escobar, M. Coleman, and T-S Chung (2011). "Polybenzimidazole Forward Osmosis Membranes Functionalized for Increased Surface Charge and Hydrophilicity," 2011 NAMS Annual Meeting, Las Vegas, NV, June 4-8, 2011.

Problem and Research Objectives:

Forward osmosis (FO) is a technology that shows great potential as an alternative to current desalination techniques. The most attractive features of a FO membrane system include lower operational cost and less energy requirement. Unlike reverse osmosis (RO), that uses hydraulic pressure to create the driving force of water permeation, FO processes use an osmotic pressure gradient between the feed and draw solutions to create the driving force across a semi-permeable membrane. Water flows through the membrane, concentrating a saline feed solution, and diluting a draw solution of much higher osmotic pressure.

While emphasis has been placed on developing FO processes recently [1], two main drawbacks still exist. Most commercially available membranes were designed for RO processes and have proven to be less than ideal for FO systems. RO membranes are built on thick fabric support layers that suffer high levels of internal concentration polarization, significantly reducing membrane flux [2]. The second drawback involves finding an economically viable and easily separable draw solute. Many draw solutes have been examined as possible candidates for FO processes including: ammonium bicarbonate, calcium chloride, potassium bicarbonate, magnesium chloride, magnesium sulfate, and sodium bicarbonate [1, 3-4]. Ammonium bicarbonate was chosen as the draw solution solute for this study due to its ease of separation to allow for feed solute rejection studies [5-6].

To address the issue of finding a suitable membrane material for FO processes, researchers in Singapore recently developed a PBI nanofiltration (NF) hollow fiber membrane [7-8]. PBI is a polymer that exhibits high mechanical strength, thermal stability, and chemical resistance [9-10]. Through use of the phase inversion technique, asymmetric PBI membranes were formed yielding high water fluxes but low monovalent salt rejection [7-8].

PBI nanofiltration membranes from these studies showed amphoteric behavior with desirable water flux and high rejection of divalent ions. Rejection of ionic species was found to be highly dependent on the solution pH. pH values determine the phases and sizes of the ionic species, in addition to the surface charge characteristics of the PBI membrane [7-8]. It was also shown through surface modification of the PBI membranes that the rejection of aqueous solutes is highly dependent on both the membrane pore size and electrostatic interaction between the solute and membrane. Analysis of virgin and modified PBI membranes in pressure driven systems with single electrolyte solutions at various pH values showed a decrease in solute permeability with modification at neutral pH values, with increasingly higher rejection as the pH increased and the membranes took on higher surface charges [11-13].

In an attempt to enhance the properties of the PBI membranes, the authors have recently demonstrated that asymmetric flat sheet PBI membranes could successfully be cast, and functionalized, using several different modifying agents [12-13]. The previous study used 4-(chloromethyl) benzoic acid (CMBA) for an activation step and p-phenylene diamine (PD), ethylene diamine (ED), and taurine to functionalize the membrane surface. All three modifications resulted in increases in hydrophilicity and membrane surface charge. Additionally, it was hypothesized that the modifications led to decreases in the mean pore size over that of the virgin sample. Previous research with PBI membranes chemically

modified with p-xylylene has shown that modification could successfully decrease membrane pore size in the selective layer to a molecular level [11]. Modification with p-xylylene [11] involves a similar reaction to the activation step with CMBA [12-13] described previously by the authors, but has two reactive chloride groups that result in cross-linking of the PBI chains.

Recent studies have indicated that improvements in the wetting of a membrane surface can be critical in improving the membranes water permeability [14]. Lack of sufficient wetting exacerbates internal concentration polarization and disrupts continuity of water throughout the membrane structure. Decreased water continuity within the internal membrane pathways reduces the effective porosity, thus reducing water transport. This study [14] showed that by RO pretreating membranes used in FO application, or through addition of surfactants to the solutions used in the FO process, water permeability could be increased due to the enhanced wetting effect, and subsequent removal of air and vapor trapped in the porous selective layer of the membrane. Each of these techniques affected the various layers of the membrane differently depending on the structure and hydrophobicity of the layer. If the membrane surface is modified to be more hydrophilic, then the wetting effect of the membrane surface can be enhanced.

The focus of this study is to investigate the performance of the functionalized flat sheet PBI membranes in a forward osmosis application. The functionalization of membranes studied included the three modifying agents used previously, and an additional fourth modifying agent, poly(acrylamide-co-acrylic acid). Poly(acrylamide-co-acrylic acid) (PAcA) was selected for this study due to its ability to crosslink with the activated PBI membrane and because of its natural properties in aqueous environments. PAcA has both amino ($-NH_2$) and carboxyl (-COOH) functional groups that can either protonate or deprotonate based on the solution pH, and it is incredibly hydrophilic in nature [15-17]. A summary schematic of the two-step chemical modification procedure is shown in Figure 1. For simplicity, the modification of the PBI repeat unit is only shown at one of the secondary amines for one of the imidazole rings. This reaction could take place at both imidazole rings for the repeat units on the membranes surface.

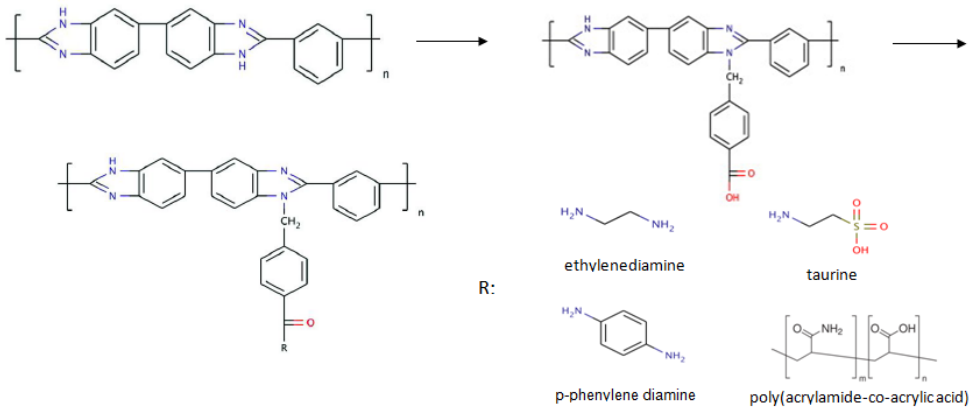

Figure 1. Chemistry for two-step modification procedure.

Methodology:

Chemicals

All chemistry required for PBI membrane casting, preparation, and surface modification used in this study has been described previously [12-13]. PBI dope was supplied by PBI Performance Products, Inc. (Charlotte, NC) as a 26 wt% solution. Ammonium bicarbonate, poly(acrylamide-co-acrylic acid), all poly(ethylene glycol) solutes, and sodium chloride were purchased from Sigma-Aldrich (USA). Glycerol, glucose, sucrose, and raffinose were purchased from Fisher Scientific (USA). DI water was supplied by a continuous distillation apparatus.

Feed and draw solutions

For all experiments the draw solution used was a 2M ammonium bicarbonate (NH_4HCO_3) solution made by dissolving reagent grade ammonium bicarbonate in DI water. The feed solutions for all experiments consisted of a 0.1M sodium chloride (NaCl) solution. The osmotic pressure gradient across the membrane was approximately 65 bar [1, 3].

Polybenzimidazole forward osmosis membranes

All PBI membranes were cast and modified in house. The casting and two-step modification procedure has been previously described [12-13]. In summary, the PBI flat sheet membranes were cast at 150 μm with a doctor's blade and formed by way of the phase inversion technique. The selective layer thickness was found to be approximately 8 μm. After formation, the surface was activated by way of reaction between the highly reactive chloride of the CMBA molecule and the secondary amine in the imidazole ring of the repeat unit in the PBI backbone. The second step involved subsequent modifications performed in a 2-(N-morpholino) ethanesulfonic acid (MES) buffer at pH 6 using N-(3-dimethylaminopropyl)-N'-ethylcarbodiimide hydrochloride (EDCH) and N-hydroxylsuccinimide (NHS) chemistry. Figure 2 shows a cross-sectional view of the asymmetric virgin PBI flat sheet membrane taken by environmental scanning electron microscopy (ESEM). An FEI Quanta 3D FEG Dual Beam Electron Microscope (FEI, U.S.A.) was used to image the sample.

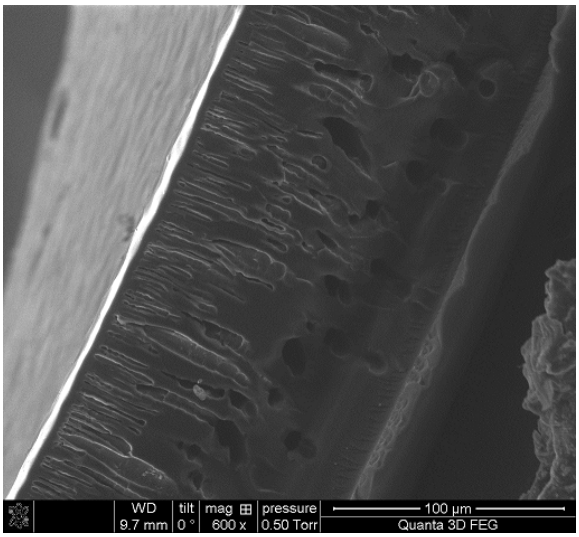

Figure 2. SEM image of the asymmetric PBI flat sheet membrane cross-section.

FTIR, contact angle, and zeta potential

The PBI membranes used in this study have previously been characterized by Fourier transform infrared spectroscopy in attenuated total reflectance mode (FTIR-ATR), contact angle, and zeta potential measurements [12-13]. FTIR analysis was obtained on a Varian Excalibur Series Fourier Transform Infrared instrument, the FTS-4000 Spectrometer and the UMA-600 Microscope (Randolph, MA). Contact angle was determined using a Tantec Model CAM-MICRO Contact Angle Meter (Tantac, Inc., U.S.A.). Surface charge was analyzed by measuring the zeta potential on the membrane surface. Samples were measured using an electrokinetic analyzer (BI-EKA, Brookhaven Instrument Corp., Holtsville, NY), located at Michigan State University. These techniques have shown the effects of PBI surface functionalization on membrane chemistry, hydrophilicity and surface charge [12-13].

Pore size determination

Total organic carbon (TOC) analysis was used to determine the pore sizes of the membranes developed. Concentrations of the solute solutions used for pore size determination were measured with a Tekmar-Dohrmann, Phoenix 8000 UV-persulfate TOC Analyzer (Tekmar Company, OH). The approach involved introducing feed solutions containing uncharged solutes (Table 1) of various Stokes-Einstein radii to the selective layer of the PBI membranes in an Amicon 8010 dead-end filtration cell (Millipore, USA). All experiments were performed as single solute permeation runs. The diluted permeate and original feed solutions were sampled in the TOC to determine solute rejection. The apparent solute rejection R (%) was calculated by Equation 1:

$$R = \left(1 - \frac{C_p}{C_f}\right) \times 100\% \qquad (1)$$

where C_p and C_f are the solute concentrations in the permeate and feed solutions, respectively. The uncharged solute samples are shown in Table 1 along with their Stokes-Einstein radii [7, 15]. Nonionic

molecules have been used to determine membrane pore sizes by previous researchers [7, 11, 18-20] and a similar procedure was followed for this study.

Table 1. Molecular weights and Stokes-Einstein radii of neutral solutes for pore size determinations.

Solute	Mw ($g\ mol^{-1}$)	Stokes radii (nm)
Glycerol	92	0.26
Glucose	180	0.37
Sucrose	342	0.47
Raffinose	504	0.58
PEG	600	0.61
PEG	1000	0.80
PEG	2000	1.41
PEG	4600	1.75
PEG	8000	2.31

200 ppm solutions were made of each individual solute in DI water. Each separation experiment involved permeation of a single solute in a pressure driven dead-end flow cell at 4.82 bar. Every membrane-solute combination was repeated three times so the average value could be calculated. The rejection values for all solutes were used to determine the mean effective pore size and the molecular weight cut-off (MWCO) for each membrane modification. The MWCO of a membrane is the molecular weight of the solute that is 90% retained by the membrane [18].

Forward osmosis operational set-up

The FO process used in this study is shown in Figure 3. The membrane filtration cell was a Sterlitech CF042 acrylic filtration cell (Sterlitech Corporation, Kent, WA) modified for forward osmosis to allow for water to flow through rectangular channels on both sides of the membrane. The channel dimensions of 8.25 cm length and 5.1 cm height provided a total membrane area of 42 cm^2. The 0.1M sodium chloride feed solution flowed across the selective (dense layer) side of the membrane and the 2M ammonium bicarbonate draw solution across the permeate side of the membrane. Polypropylene mesh feed spacers were used in the channels to provide membrane support and to enhance turbulence and mass transport. Variable speed peristaltic pumps (Fischer Scientific) were used to pump the liquids in co-current flow and at equal flow rates. Due to the endothermic disassociation of ammonium bicarbonate, the draw solution was allowed to equilibrate to room temperature before the FO experiments were begun. The solution was continuously mixed during the equilibration period. Both the feed and draw solutions were run at room temperature for all experiments.

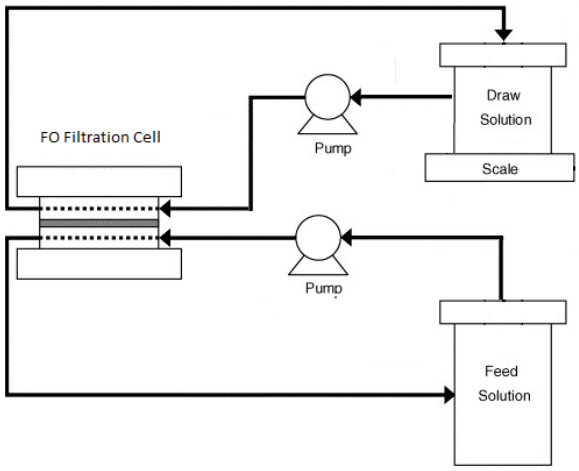

Figure 3. Schematic of co-current flow forward osmosis system.

This experimental set-up allowed for minimization of strain to the membrane as a result of unequal pressure across the length of the membrane; and to reduce the effect that additional parameters (temperature gradient, different fluid velocities, counter-current flow, etc.), other than concentration gradient, would have on the transport of feed solution across the membrane.

The initial experimental approach involved testing a 2M ammonium bicarbonate solution against feed solutions of 0.1M sodium chloride solutions, at both pH 7 and pH 10. The pH adjustments were made with concentrated sodium hydroxide solution. The flow rates of both the feed and draw solution were approximately 65 mL/min. The osmotic pressure gradient between the bulk feed and draw solutions was approximately 65 bar [1, 3].

Transport properties

Mass transport across the membrane was determined by measuring the weight change of the draw solution in one hour intervals over a five hour period. The weight of the draw solution increases as water permeates across the membrane from the feed solution by way of osmosis. The volumetric increase divided by the membrane area and the selected time period gives the water flux.

Sodium chloride transport was determined by taking a sample of draw solution, after a complete FO run, and boiling the solution until the solvent had completely evaporated. The boiling process resulted in the decomposition of ammonium bicarbonate into ammonia and carbon dioxide gases [5-6] leaving only sodium chloride and sodium hydroxide crystals remaining. The weight of the remaining crystals was measured after boiling, and the crystals were then diluted with a known volume of DI water after which the pH and conductivity were measured. The concentrations of sodium chloride solutions were measured with a conductivity meter. All solution pH values were measured with a Corning 430 glass pH-electrode and a pH meter (Corning, NY). Pure water permeability from a pressure driven process at 4.82 bar was reported previously by the authors [12-13] and were used for comparison.

In order to determine the true rejection of the chloride ion by the selective layer of the PBI membranes tested, a chloride selective electrode would be needed. However, since this was not available, a second approach involving calculating the sodium hydroxide concentration from the pH measurements of the diluted salt solutions was used. The weight of the sodium hydroxide present was determined and subtracted from the total weight of the dried salt permeate weighed before dilution. The weight of the sodium chloride sample could then be divided by the weight of the water permeate and presented as the weight fraction to be compared against the other membranes.

Principal Findings:

Membrane characterization

The FTIR-ATR spectrum for PBI and the functionalized membranes (Figure 4 and Table 2) is described in detail in Hausman et al [13] for the modifications using ED, PD, and taurine. PAcA modification is confirmed by the C=O band around 1620cm^{-1} , the band around 1645cm^{-1} associated with the N-H and NH_2 bonds, and the alkane stretch around 2900cm^{-1}. The use of this technique verified the successful modification for the CMBA surface activation and and for each of the final membrane modifications.

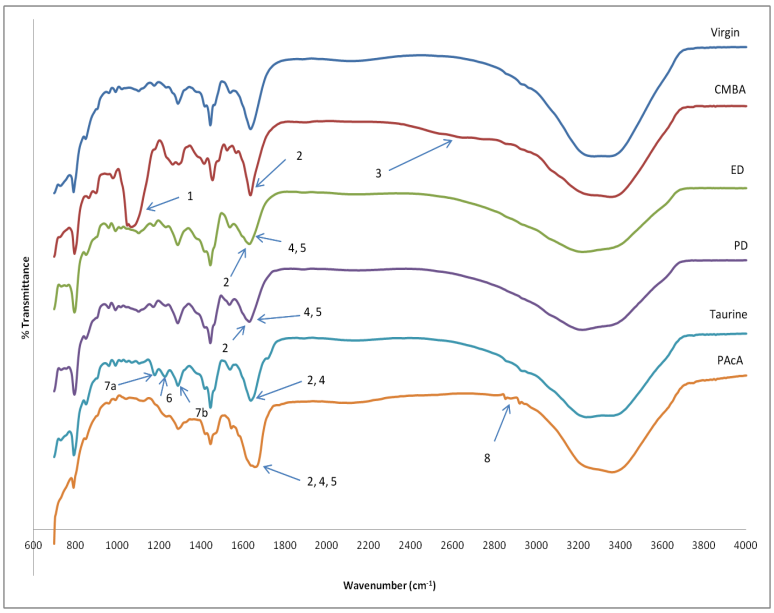

Figure 4. FTIR results for all membrane samples.

Table 2. FTIR functional group location.

Number	Functional group	Wave number (cm^{-1})
1	C–O	1057
2	C=O	1620–1640
3	OH	~ 2670
4	Secondary amine N–H	1645
5	Primary amine NH_2	1645
6	S=O	1215
7a	SO_2 (symmetrical)	1168
7b	SO_2 (anti-symmetrical)	1285
8	Alkane stretch C-H	2850-3000

Zeta potential

In previous studies [12-13] using the modification technique discussed here the final surface modifications for p-phenylene diamine, ethylene diamine, and taurine showed more charged surfaces than the virgin PBI membranes. The addition of poly(acrylamide-co-acrylic acid) for use in this study is expected to yield an even higher surface charge than the other modifications. PAcA has both amino (-NH_2) and carboxyl (-COOH) functional groups that can either protonate or deprotonate based on the solution pH. In this study the pH of the feed and draw solutions for all runs equilibrated to approximately 8.3. At this pH value it is expected the carboxyl groups on the PAcA membranes would be deprotonated to a significant degree (isoelectric point around 4.75) [15-16]. A membrane with a negative surface charge is expected to have a high rejection of anionic species in the feed solution.

Contact angle

Contact angle measurements for the virgin, CMBA activated, and all final modifications are shown in Figure 5. The hydrophilicity increased for all membrane modifications.

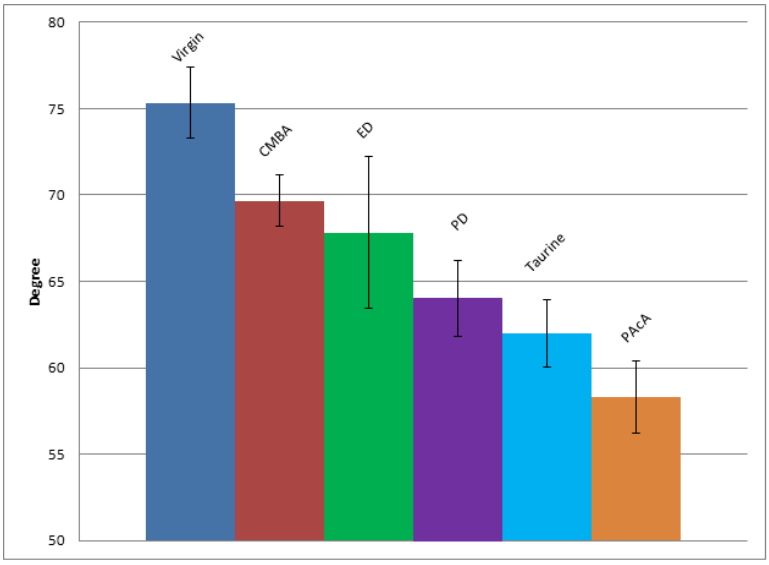

Figure 5. Contact angle measurements for all membrane samples.

Pore size determination

Table 3 shows the mean pore radius, the molecular weight cut-off, and the pore radius where the molecular weight cut off is reached. The effective mean pore sizes of all virgin and modified membranes fall in the nanofiltration range (0.5-2 nm in diameter) [7]. The effective mean pore radius of the unmodified membrane was 0.61 nm.

Table 3. Pore size data

	Virgin	CMBA	ED	PAcA	Taurine	PD
Mean radii (nm)	0.61	0.45	0.38	0.41	0.37	0.33
MWCO (Da)	7977	4161	1994	1399	1287	886
MWCO radii (nm)	2.31	1.66	1.14	0.95	0.91	0.75

From Table 2 it is observed that every membrane modification showed a reduced pore size over that of the virgin. Additionally, all the final modifications showed reduced pore sizes over the CMBA activated. The ED membrane had a smaller mean pore size than the PAcA but a larger MWCO. This is believed to be attributed to the large size (M_w = 5,000,000) and cross-linking ability of the PAcA. If the large PAcA molecules are bonding to multiple sites across the membrane surface in random order, the effects of steric exclusion are expected to be more pronounced on larger solutes [18-20]. As expected the taurine and PD molecules resulted in smaller pore sizes than the ED. They also showed smaller pore sizes than the PAcA. The smaller pore sizes of the PD and taurine modifications over the PAcA are believed to due to the smaller size of these modifying agents. The PD and taurine are small enough to permeate the pores of the activated membrane and react to a greater degree than the PAcA. The large size of the PAcA molecules restricts them from penetrating into the membranes pores. The effective mean pore size and MWCO for each membrane sample was calculated from a polynomial equation of the third degree. The typical rejection curves for uncharged solutes (Table 1) followed s-shaped rejection curves [18] that were analyzed with polynomial trendlines.

Forward osmosis flux results

While water permeability through all the modified membranes was lower than that of the virgin membranes in pressure-driven mode (Figure 6), water permeability through all modified membranes was greater than permeability through the virgin membranes in FO mode (Figure 7). Figure 7 shows the results of the FO flux data measured for all the membranes where the starting pH of the feed was 7. Each membrane modification was run three separate times to determine average membrane flux values. Relating this to the pure water flux data obtained for the process driven by hydraulic pressure, (pressure-driven nanofiltration process, Figure 6), it was observed that the behavior of the membranes was reversed. In the pressure-driven process [12-13], the driving force for water permeation was the hydraulic pressure (4.82 bar) applied to the membrane. In the pressure driven process, the primary resistance to water flux stemmed from the membrane morphology: mean pore size, pore size distribution, tortuosity, membrane thickness, etc. The CMBA pure water flux was found to be approximately 30% lower than the virgin membrane flux and the modified samples were all found to be 50-60% lower than the CMBA, or 65-75% lower than the virgin.

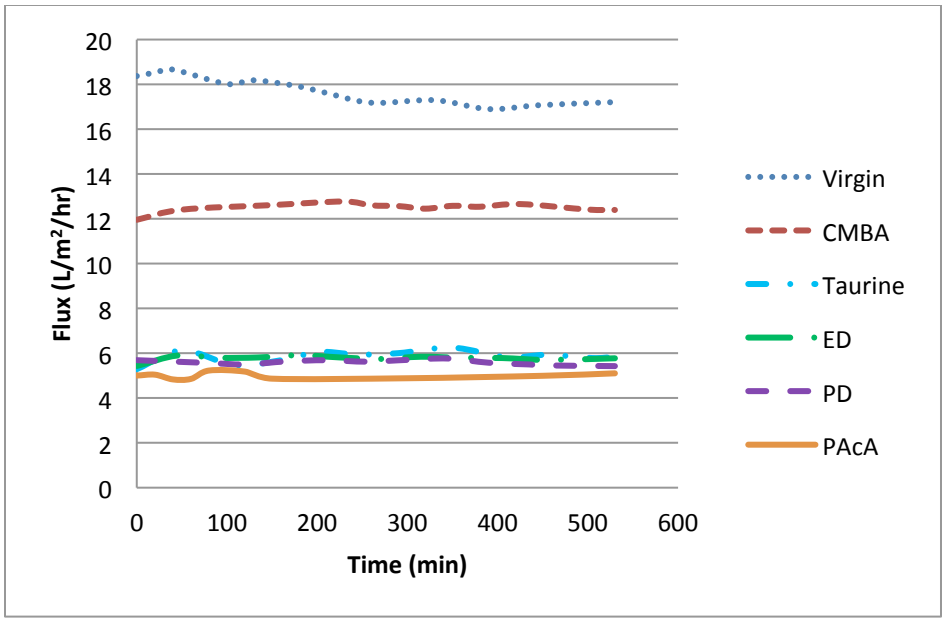

Figure 6. Flux data for all membranes in pressure driven system.

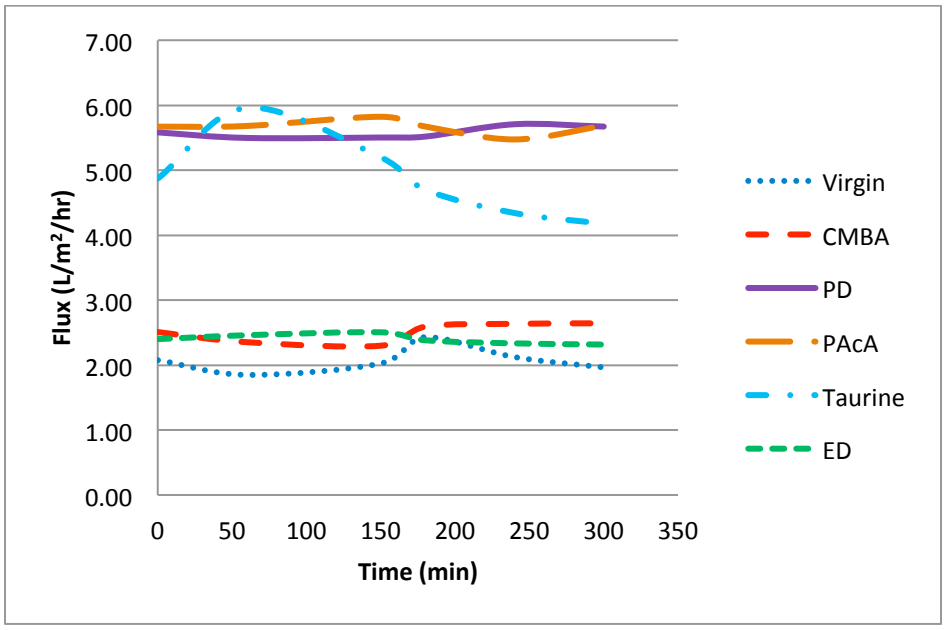

Figure 7. Flux data for all membranes in FO system

The results of the FO experiments were the reverse of those in the pressure driven experiments. The two membranes with the lowest flux in the dead-end cell were the PD and PAcA membranes. In the FO process these were the two membranes with the highest flux results. The virgin flux results were 63% and 64% lower than the PD and PAcA, respectively. The virgin was 17% lower than the CMBA and the CMBA was 55% and 56% lower than the PD and PAcA, respectively. The ED and CMBA flux values were very close to one another and not much higher than the virgin. The taurine modified membranes showed an early flux close to the PD and PAcA but began to drop lower as the run time progressed.

The performance of the membranes in FO, as opposed to the pressure driven experiments, was primarily believed to be attributed to the increased hydrophilicity of the modified membranes. In pressure driven experiments, water is forced through the membrane by hydraulic pressure, where-as in the FO system the water solution flows freely past the membrane surface. The increase in hydrophilicity of the modified membranes caused the system to favor water transport. Contact angle measurements for each of the membranes, shown in Figure 5, displayed an increased hydrophilicity after functionalization.

The contact angle for the ED membrane was the highest of the modified samples, and ED had the lowest water flux of the final modifications. Additionally, ED was the smallest of the modifying agents, but still caused a 38% decrease in the membrane pore size. The CMBA activation caused a 25% decrease. Since the hydrophilicity was slightly higher with a smaller pore size, this could explain the similar water flux between the ED and CMBA membranes. Additionally, the mean ED contact angle value was lower than the CMBA but the standard deviation was the largest and actually overlapped the lower end of the virgin standard deviation.

Despite the similar water fluxes, the weight fraction of sodium chloride in the permeate was significantly lower for the ED membranes. Previous work has shown zeta potential results for the ED modified membrane with a higher surface charge than the CMBA [12-13]. The higher surface charge and reduced pore size seems to explain the lower weight fraction of sodium chloride in the permeate while the water flux remains roughly the same as the CMBA membrane.

It is interesting to note that water transport was far lower in the FO system than the pressure-driven cell. The osmotic pressure gradient between the two bulk solutions was roughly 65 bar [1, 3], whereas the hydraulic pressure in the pressure-driven cell was only 4.82 bar. This behavior was expected and has been reported previously. Low flux results in FO systems were the result of internal concentration polarization [1-4]. Concentration polarization reduces the osmotic pressure gradient across the membrane to the point where it is significantly lower than that of the bulk. This affects the performance of the trans-membrane water transport, resulting in much lower water flux across the membrane than would be expected from the bulk osmotic pressure gradient.

Salt permeability

Due to the buffering effect of ammonium bicarbonate and sodium bicarbonate, the pH of the draw and feed solutions for the FO experiments equilibrated to a slightly basic value (approximately 8.3) where all the membranes were expected to have some degree of surface charge [12-13]. From the previous zeta potential studies involving virgin, CMBA activated, taurine, ED and PD modified at pHs 7 and 10, the readings were approximately 1.7, 4.2, -0.4, -4.5, and -7.2 mV, respectively for pH 7 and 0.1, 4.2, -3.7, -7.3, and -11.5 mV, respectively for pH 10. The rejection of 0.1M sodium chloride solutions for all modified membranes in the FO system was significantly higher than the virgin.

In a typical membrane filtration system, the percent rejection is quantified by determining the concentration of salt in the feed solution, and the concentration of the salt that permeates the membrane. Since the relationship between concentration and conductivity of sodium chloride is linear,

concentration can be determined by taking conductivity measurements of the feed initially and of the draw solution after the ammonium bicarbonate has been removed. Use of this technique would not be ideal for the process used for this discussion because the rejection values would be for a bench scale system where both the feed and draw solutions were recycled past the membrane many times over. For the 65 mL/min flow rate selected for both streams, the 1000 mL draw solution was recycled past the membrane roughly 19.5 times over a five-hour period. With 19.5 turnovers per experiment, the percent rejection values were deemed subjective. The most relevant technique for relating salt permeate data in this system is with the salt weight fractions measured for each membrane. This way, the performances of the membrane modifications can be related to one another and the virgin.

Figure 8 shows the transport ratios for the weight fraction of the sodium chloride and sodium hydroxide per water permeating the membranes, and the weight fraction of sodium chloride that permeated through the membranes. The thin bar in the back is the weight fraction of the total salt content remaining after the solvent boil off and the thicker bar in the front is the weight fraction for just the sodium chloride. From Figure 8, it is clear that every modified surface yielded higher rejection of sodium chloride over that of the virgin. The surface charges of the modified membranes were greater than the virgin at these slightly basic pH values. Additionally, the pore sizes of the modified membranes were smaller and resulted in better rejection. Due to the hygroscopic nature of sodium hydroxide and sodium chloride, the weight readings of the dried salt samples were not entirely accurate. As the heated beaker and remaining salt sample were left to cool some water moisture was trapped and added to the final weight. While the inaccuracy of the salt measurements may negate this as quantitative data, the weight measurements do provide excellent qualitative data to compare the modified samples to one another and to the unmodified.

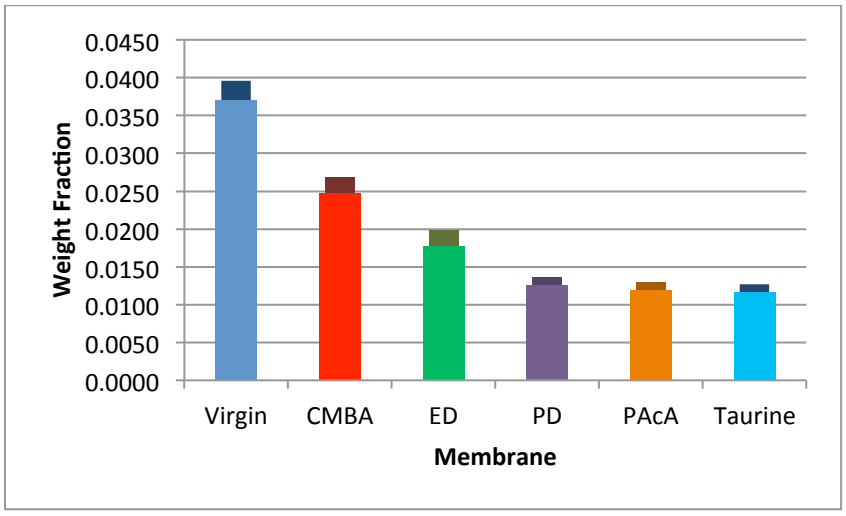

Figure 8. Total salt (back, thin bar) and sodium chloride (front, thick bar) weight fractions for each membrane.

pH effects

It was clear after only a few experimental runs that testing a feed solution at pH 10 was an impractical endeavor since the buffering strength of the much more concentrated ammonium bicarbonate draw

solution equilibrated the pH of both feed and draw solution streams. This effect was observed because both the feed and draw solutions were recycled past the membrane surface, resulting in several turnovers of the process volumes. In addition, one experiment was attempted to bring the draw solution pH up to 10, using ACS grade ammonium hydroxide, but resulted in such a large dilution that the approach was discredited. To bring the pH of 1L of draw solution to 9.98 required 400mL of ACS grade ammonium hydroxide (28-30%), diluting the solution to only 1.43M ammonium bicarbonate, and lowering the osmotic pressure gradient to approximately 47 bar. In a true desalination process, the feed solution would not be recycled past the membrane, and the pH equilibration would not be as prevalent. Even after this experiment however, when the solutions were boiled down and rehydrated to determine sodium chloride rejection, the pH of the final salt solutions of both the feed and draw followed the same trend as seen with all the other samples.

It was observed for all membrane-pH samples that after the five hour run time, the pH of both feed and draw solutions were equilibrated. Previous studies have shown high rates of reverse salt diffusion for ammonium bicarbonate draw solutions [3-4]. For the samples where there was no pH adjustment for either the feed or draw solutions, and also for the samples where the feed was adjusted to pH 10, the final pH of the feed and draw solutions was always between 8.2-8.4 (this pH range is resultant of the presence of sodium bicarbonate and sodium carbonate which buffer in this pH range). For the experiment with both feed and draw pH values initially around 10, both streams remained around 10.

At the end of a full FO run, a known volume of draw solution was boiled down until all the water evaporated. During this boiling process, all the dissolved ammonium salts decompose into ammonia and carbon dioxide. The remaining solid was then diluted with DI water to the original volume, so information about the salt rejection and membrane performance could be obtained. All the membrane experiments, including the experiment where the initial pH values were both at 10, followed the same behavior. After the boil off, and subsequent dilution, the pH of the draw solution was over 10, and the pH of the feed solutions was neutral.

These results indicate membrane selectivity of the sodium ions over the chloride ions in the feed stream. This membrane behavior was expected for the slightly basic environment where the membrane takes on a negative surface charge. In addition to surface charge, the anionic species are larger than the cationic. The larger size of the anions leads to an increased size exclusion effect from the dense membrane structure. Considering the pH equilibration for the readings taken immediately after the five-hour experimentation time, but the large pH discrepancy after the solutions were boiled down and diluted, it seems the membrane allowed passage of sodium and ammonium ions much more freely than their anion counterparts.

The selectivity of the membrane for sodium ions was balanced by the reverse diffusion of the small and positively charged ammonium ions, thus obeying the electroneutrality principle. The excess of sodium ions permeating the PBI membranes yielded the higher pH values in the diluted draw solutions. When the draw solution was boiled down the ammonium and bicarbonate ions degrade into ammonia, carbon dioxide, and water. The remaining solute crystals, after completion of boiling, were a mixture of sodium chloride and sodium hydroxide. In the feed solution however, the thermal decomposition of the ionic

species leads to a breakdown of all the ammonium and bicarbonate ions. The excess ammonium and chloride ions decomposed into ammonia and hydrogen chloride. With the continued heating, the hydrogen chloride was also boiled off as vapor, and the remaining salt was simply sodium chloride. The pH of the diluted salt solution for the feed was thus neutral.

This pH phenomenon is a qualitative confirmation of the membranes selectivity for the cationic species, and higher rejection of the anionic species. The higher rejection was attributed to both steric exclusion and Donnan exclusion. The presence of sodium hydroxide in the diluted solution gave an elevated conductivity reading, and thus shows a lower sodium chloride rejection value when conductivity readings are taken. If conductivity readings were used solely to measure salt rejection then the percent rejection values would appear far lower than the actual values.

Significance:

The overall lower mass transport across the virgin membrane in FO mode, despite the larger pore sizes, was believed to be due to the membranes higher hydrophobicity. All the modified membranes were more hydrophilic than the unmodified samples. The more hydrophilic surfaces should undergo an increased wetting effect, where the membrane-fluid interactions favored water transport. In addition to the effect of the more hydrophilic surfaces, the charged membrane surfaces showed a higher degree of sodium chloride rejection when examined as weight fractions of the permeate transporting through the membranes.

The results of PBI surface functionalization with the intent to increase hydrophilicity, increase surface charge, and decrease the membrane pore size show enhanced membrane performance both with respect to water flux and salt rejection. The reduced pore size coupled with the use of a feed stream carrying divalent or larger ions mixed with colloidal particles may have the ability to yield excellent results and high purity water. In addition, if the cations chosen were much larger (e.g. transition metals or contaminants in industrial wastewaters) then the overall salt rejection would be expected to increase.

References:

1. T.Y. Cath, A.E. Childress, M. Elimelech, Forward Osmosis: Principles, applications, and recent developments, J. Membr. Sci. 281 (2006) 70-87

2. J.R. McCutcheon, M. Elimelech, Influence of concentrative and dilutive internal concentration polarization on flux behavior in forward osmosis, J. Membr. Sci. 284 (2006) 237-347

3. N.H. Hancock, T.Y. Cath, Solute coupled diffusion in osmotically driven processes, Environ. Sci. and Technol., 43 (2009) 6769-6775

4. A. Achilli, T.Y. Cath, A.E. Childress, Selection of inorganic-based draw solutions for forward osmosis applications, J. Membr. Sci. 364 (2010) 233-241

5. J.R. McCutcheon, R.L. McGinnis, M. Elimelech, A novel ammonia-carbon dioxide forward (direct) osmosis desalination process, Desalination 174 (2005) 1-11

6. J.R. McCutcheon, R.L. McGinnis, M. Elimelech, Desalination by ammonia-carbon dioxide forward osmosis: Influence of draw and feed solution concentrations on process performance, J. Membr. Sci. 278 (2006) 114-123

7. K.Y. Wang, T.S. Chung, J.J. Qin, Polybenzimidazole (PBI) nanofiltration hollow fiber membranes applied in forward osmosis process, J. Membr. Sci. 300 (2007) 6-12

8. J.L. Lv, K.Y. Wang, T.S. Chung, Investigation of amphoteric polybenzimidazole (PBI) nanofiltration hollow fiber membrane for both cation and anions removal, J. Membr. Sci. 310 (2008) 557-566

9. L.C. Sawyer, R.S. Jones, Observations on the structure of first generation polybenzimidazole reverse osmosis membranes, J. Membr. Sci. 20 (1984) 147

10. K.D. Kreuer, A. Fuchs, M. Ise, M. Spaeth, J. Maier, Imidazole and parazole-based proton conducting polymers and liquids, Electrochim. Acta. 43 (1998) 1281

11. K.Y. Wang, Y. Xiao, T.S. Chung, Chemically modified polybenzimidazole nanofiltration membrane for the separation of electrolytes and cephalexin, Chem. Eng. Sci. 61 (2006) 5807-5817

12. M. Flanagan, R. Hausman, B. Digman, I.C. Escobar, M. Coleman, T.S. Chung, Surface Functionalization of Polybenzimidazole Membranes to Increase Hydrophilicity and Charge, Mod. Appl. in Membr. Sci. and Technol. 18 (2011) 303-321

13. R. Hausman, B. Digman, I.C. Escobar, M. Coleman, T.S. Chung, Functionalization of polybenzimidizole membranes to impart negative charge and hydrophilicity, J. Membr. Sci. 363 (2010) 195-203

14. J.R. McCutcheon, M. Elimelech, Influence of membrane support layer hydrophobicity on water flux in osmotically driven membrane processes, J. Membr. Sci. 318 (2008) 458-466

15. E. Turan, T. Caykara, Swelling and network parameters of pH-sensitive poly(acrylamide-co-acrylic acid) hydrogels, J. of Appl. Polym. Sci. 106 (2007) 2000-2007

16. A. Thakur, R.K. Wanchoo, P. Singh, Structural parameters and swelling behavior of pH sensitive poly(acrylamide-co-acrylic acid) hydrogels, Chem. Biochem. Eng. Q. 2 (2011) 181-194

17. A. Jha, S. Agrawa, A. Mishra, J.P. Rai, Synthesis, characterization and flocculation efficiency of poly(acrylamide-co-acrylic acid) in tannery waste-water, Iran. Polym. J. 10 (2001) 85-90

18. C.M. Tam, A.Y. Tremblay, Membrane pore characterization – comparison between single and multicomponent solute probe techniques, J. Membr. Sci. 57 (1991) 271-287

19. S. Singh, K.C. Khulbe, T. Matsuura, P. Ramamurthy, Membrane characterization by solute transport and atomic force microscopy, J. Membr. Sci. 142 (1998) 117-127

20. S. Lee, G. Park, G. Amy, S.K. Hong, S.H. Moon, D.H. Lee, J. Cho, Determination of membrane pore size distribution using the fractional rejection of nonionic and charged macromolecules, J. Membr. Sci. 57 (1991) 271-287

Development of Carbon Nanotube-based Biosensor for Monitoring Microcystin-LR in water

Basic Information

Title:	Development of Carbon Nanotube-based Biosensor for Monitoring Microcystin-LR in water
Project Number:	2011OH291O
Start Date:	5/1/2011
End Date:	4/30/2012
Funding Source:	Other
Congressional District:	1
Research Category:	Engineering
Focus Category:	Water Quality, Toxic Substances, Methods
Descriptors:	
Principal Investigators:	Dionysios Dionysiou

Publications

1. Doepke Amos; Changseok Han, Tyson Back, Wondong Cho, Dionysios D. Dionysiou, Vesselin Shanov, H. Brian Halsall, William R. Heineman, Analysis of the electrochemical oxidation of multi-walled carbon nanotube tower electrodes in sodium hydroxide, Accepted to Electroanalysis.
2. Han Changseok; Amos Doepke, Wondong Cho, Vlassis Likodimos, Armah A. de la Cruz, Tyson Back, William R. Heineman, H. Brian Halsall, Vesselin N. Shanov, Mark J. Schulz, Polycarpos Falaras and Dionysios D. Dionysiou, Multi-Walled Carbon Nanotubes-based Biosensor for Monitoring Microcystin-LR in Drinking Water Sources, In preparation for submission, May 2012.
3. Han Changseok; Amos Doepke, Wondong Cho, Armah A. de la Cruz, William R. Heineman, H. Brian Halsall, Vesselin N. Shanov, Mark J. Schulz, Vlassis Likodimos, Polycarpos Falaras, and Dionysios D. Dionysiou, 2012, Multi-walled Carbon Nanotubes-based Biosensor for Monitoring Cyanotoxins in Drinking Water Sources. Oral Presentation at the 243rd American Chemical Society (ACS) National Meeting, Symposium on Environmental Applications and Ecological Implications of Nanotubes, Nanowires, and Fullerenes, Division of Environmental Chemistry, paper 528, March 25-29, 2012, San Diego, California.
4. Han Changseok; Amos Doepke, Wondong Cho, Armah A. de la Cruz, William R. Heineman, H. Brian Halsall, Vesselin N. Shanov, Mark J. Schulz, Vlassis Likodimos, Polycarpos Falaras and Dionysios D. Dionysiou, 2011, Carbon Nanotubes-based Biosensor for Detecting Cyanotoxins in Water. Poster Presentation at the 3rd International Conference from Nanoparticles and Nanomaterials to Nanodevices and Nanosystems (IC4N-3), June 26-30, 2011, Crete Island, Greece.

Development of Carbon Nanotube-based Biosensor for Monitoring Microcystin-LR in water

(USGS Annual Report FY 2011/2012)

Title:	**Development of Carbon Nanotube-based Biosensor for Monitoring Microcystin-LR in water**
Project Number:	
Start Date:	05/01/2011
End Date	4/30/2012
Funding Source	104(b)
Congressional District:	1
Research Category:	Engineering
Focus Category:	Water Quality; Water Supply; Toxic Substances
Descriptors:	None
Principal Investigator:	Dionysios D. Dionysiou

Principal Investigator
Dr. Dionysios (Dion) D. Dionysiou, Professor
Environmental Engineering and Science Program
School of Energy, Environmental, Biological, and Medical Engineering
University of Cincinnati, Cincinnati, OH 45221-0012
Email: dionysios.d.dionysiou@uc.edu
Fax: +1-513-556-2599; Tel: +1-513-556-0724

Collaborators:
Dr. Vesselin Shanov (Energy and Materials Engineering), Dr. Mark Shultz (Mechanical Engineering), Dr. William Heineman (Chemistry),
University of Cincinnati, Cincinnati, OH

1. A completion report

The occurrence of blue-green algae, a.k.a. cyanobacterial blooms, has increased in freshwater lakes, basins, rivers and ponds throughout the world including America [1, 2], Argentina [3], Australia [4], Spain [5], Uganda [6], and China [7] due to the eutrophication and warm temperature of surface water. In the summer of 2010, blue-green algae blooms with excessive concentration of microcystin toxin occurred and warnings were issued in 20 public lakes and ponds across the state of Ohio, including Grand Lake St. Mary, Ohio's largest inland lake. The level of microcystins (MCs) ranged from 5.4 μg/L to 67.3 μg/L in several freshwater reservoirs and inland lakes in Ohio [8]. In addition, in November, 2010, the USEPA issued new standards for protection of Florida waters in order to keep clean water safe from HABs pollution [9]. In California, the death of sea otters by microcystin toxin from freshwater was reported in September, 2010 [10]. Australia also issued a guideline to protect public health from the threat of toxins, which were released from blue-green algae in 2010 [11]. In recent research, Graham et al. obtained samples from cyanobacterial blooms in 23 Midwestern United State lakes to evaluate potential human health risks and reported that 96% of blooms contained toxin-producing cyanobacteria such as *Aphanizomenon*, *Cylindrospermopsis*, and *Microcystis*. In particular, microcystins, which are deleterious hepatotoxins, were found in all blooms [1]. Among the hepatotoxins, MCs are the most commonly reported cyanotoxins and MC-LR is the most frequently occurring variant among MCs in the United States and throughout the world [12-14]. The LD_{50} values of MC-LR for mouse bioassay and brine shrimp assay are 25-150 μg/kg and 5-10 mg/L, respectively [15]. The provisional concentration limit of MC-LR in drinking water of 1 μg/L was assigned by the World Health Organization (WHO) [16]. Current methods to detect MC-LR in various matrices require long processing times, sophisticated instruments, complex procedures and high expenses. A sensitive, specific, and simple method for monitoring MCs is necessary to immediately institute remedial measures to prevent exposure to these toxins. To this end, carbon nanotubes' electrical and physical properties (e.g. high electrical conductivity, huge electrochemically active surface area, and broad working area) are desirable for developing novel submicron sized electrochemical sensors. An innovative, field-portable, continuously monitoring multi-walled carbon nanotube (MWCNT)-based biosensor can detect MC-LR at low detection limits. During this period of the project (May 1, 2011 through April 30, 2012), various research activities were conducted to develop MWCNT-based biosensor for monitoring of a cyanobacterial toxin, MC-LR.

1.1 Research Objectives

The physical and electrochemical properties (e.g. high electrical conductivity, ease of functionalization, huge electrochemically active surface area, and broad working area) of MWCNTs make them a candidate material for the development of electrochemical

biosensors/immunosensors. Electrochemical biosensors using antibodies are also very promising for on-site monitoring of MC-LR due to the high selectivity, low expenses, and simplicity of the detection method. The objectives of the project were to investigate the methods/procedures to fabricate MWCNT-based electrode and functionalize the interface of MWCNT for sensing applications and investigate the method of integration between monoclonal antibodies/protein phosphatases and MWCNT to achieve specificity of toxin identification as well as to develop, characterize, and evaluate sensor performance for identification of MC-LR.

1.2 Methodology and Findings

In this study, we reported three main findings. Firstly, dense arrays of MWCNT were synthesized in controlled shapes by using a patterned catalyst with water-assisted chemical vapor deposition (CVD). The MWCNT-based electrodes were fabricated with a grown MWCNT array. The electrodes were functionalized with potentiostatic treatment in alkaline solution in order to produce polar groups on the interface of MWCNT array for the cross-linking reaction with cross-linking agents and immobilization of biomolecules. The electrochemical properties of MWCNT electrodes were characterized with cyclic voltammetry, micro-Raman spectroscopy, X-ray photoelectron spectroscopy (XPS), optical microscopy, and electrochemical impedance spectroscopy (EIS) before and after functionalization. Cyclic voltammetry of fabricated electrodes shows well-defined redox peaks in the presence of redox species before and after functionalization, which indicates MWCNTs are a suitable candidate as a sensing material. From the micro-Raman analysis, the higher the intensity ratio of the D to the G-band the more functional groups (i.e. defects in the graphitic structure or even amorphous carbon) are formed on the MWCNTs after functionalization, thus indicating that the functionalization process is indeed effective. In addition, the increase of oxygen species and ratio of a C-C:C=O after the functionalization in XPS analysis corroborated the micro-Raman analysis for the functionalization. Secondly, the MWCNT-based biosensors were prepared by immobilization of MC-LR onto the functionalized MWCNT array electrodes. The change of electron-transfer resistance of prepared biosensors following the conjugation process using MC-LR and antibody was measured with EIS in order to show the efficient sensing properties of the MWCNT-based biosensor as electrochemical biosensors. The increase of the electron-transfer resistance with the process of MC-LR and antibody conjugation through the electrochemical impedance spectroscopy study indicated the proposed technique is very useful for monitoring of

MC-LR. Finally, the calibration curve was established by using the change of electron-transfer resistance using different concentration of MC-LR. The difference of electron-transfer resistance was greater at lower concentration of MC-LR. The working range of MWCNT based biosensor was from 0.05 to 20 $\mu g \cdot L^{-1}$. The WHO provisional concentration limit (1 $\mu g \cdot L^{-1}$) [16] is much higher than our calculated method detection limit of 0.04 $\mu g \cdot L^{-1}$.

References:

[1] Graham, J.L, Loftin, K.A., Meyer, M.T., and Ziegler, A.C. (2010) Cyanotoxin Mixtures and Taste-and-Odor Compounds in Cyanobacterial Blooms from the Midwestern United States, *Environ. Sci. Technol*. **44**, 7361–7368.

[2] Rinta-Kanto, J. M. and Wilhelm, S. W. (2006) Diversity of Microcystin-Producing Cyanobacteria in Spatially Isolated Regions of Lake Erie, *Appl. Environ. Microb.* **72**, 5083-5085.

[3] Amé, M. V., Díaz, M., and Wunderlin, D. A. (2003) Occurrence of Toxic Cyanobacterial Blooms in San Roque Reservoir (Córdoba, Argentina): A Field and Chemometric Study, *Environ. Toxicol.* **18**, 192-201.

[4] Hoeger, S. J., Shaw, G., Hitzfeld, B. C., and Dietrich, D. R. (2004) Occurrence and elimination of cyanobacterial toxins in two Australian drinking water treatment plants, *Toxicon* **43**, 639-649.

[5] Moreno, I., Repetto, G., Carballal, E., Gago, A., and Cameán, A. M. (2005) Cyanobacteria and microcystins occurrence in the Guadiana River (SW Spain), *Intern. J. Environ. Anal. Chem.* **85**, 461-474.

[6] Okello, W., Portmann, C., Erhard, M., Gademann, K., and Kurmayer, R. (2010) Occurrence of microcystin-producing cyanobacteria in Ugandan freshwater habitats, *Environ. Toxicol.* **25**, 367-380.

[7] Dai, R., Liu, J., Qu, J., Ru, J., and Hou, Y. (2008) Cyanobacteria and their toxins in Guanting Reservoir of Beijing, China, *J. Hazard. Mater.* **153**, 470-477.

[8] http://newstalkradiowhio.com/localnews/2010/12/bluegreen-alge-warning-lifted.html
http://www.ohio.com/news/103478809.html
http://www.ohoi.com/news/109308424.html
http://www.ohoi.com/news/105364543.html
http://www.dispatch.com/live/conten/local_news/stroies/2010/08/10/toxic-algae0close-anotherlake-in-ohio,html

[9] http://yosemite.epa.gov/opa/admpress.nsf/2ac652c59703a4738525735900400c2c/2b22297bbde21b4b852577dc00500960!OpenDocument

[10] http://www.physorg.com/news203595019.html

[11]http://www.environment.act.gov.au/water/water_quality/blue-green_algae_monitoring

[12] Xia, Y., Deng, J., and Jiang, L. (2010) Simple and highly sensitive detection of hepatotoxin microcystin-LR via colorimetric variation based on polydiacetylene cesicles, *Sensors and Actuators B* **145**, 713-719.
[13] Lawton, L.A., Chambers, H., Edwards, C., Nwaopara, A.A., and Healy, M. (2010) Rapid detection of microcystins in cells and water, *Toxicon* **55**, 973-978.
[14] Sangolkar, L.N., Maske, S.S., and Chakrabarti, T. (2006) Methods for determining microcystins (peptide hepatotoxins) and microcystin-producing cyanobacteria, *Water Research* **40**, 3485-3496.
[15] McElhiney, J. and Lawton, L.A. (2005) Detection of the cyanobacterial hepatotoxins microcystins, Toxicology and Applied Pharmacology **203**, 219-230.
[16] World Health Organization (1998) Guidelines for Drinking-Water Quality, 2nd ed. Addendum to Vol. 1. Recommendations, Geneva, World Health Organization, pp. 13-14.

2. Publication citations

I. Journal Articles

(1) Amos Doepke, Changseok Han, Tyson Back, Wondong Cho, Dionysios D. Dionysiou, Vesselin Shanov, H. Brian Halsall, William R. Heineman, Analysis of the electrochemical oxidation of multi-walled carbon nanotube tower electrodes in sodium hydroxide, *Accepted to Electroanalysis.*

(2) Changseok Han, Amos Doepke, Wondong Cho, Vlassis Likodimos, Armah A. de la Cruz, Tyson Back, William R. Heineman, H. Brian Halsall, Vesselin N. Shanov, Mark J. Schulz, Polycarpos Falaras and Dionysios D. Dionysiou, Multi-Walled Carbon Nanotubes-based Biosensor for Monitoring Microcystin-LR in Drinking Water Sources, *In preparation for submission, May 2012*.

II. Presentations

(1) Changseok Han*, Amos Doepke, Wondong Cho, Armah A. de la Cruz, William R. Heineman, H. Brian Halsall, Vesselin N. Shanov, Mark J. Schulz, Vlassis Likodimos, Polycarpos Falaras, and Dionysios D. Dionysiou, Multi-walled Carbon Nanotubes-based Biosensor for Monitoring Cyanotoxins in Drinking Water Sources. Oral Presentation at the 243rd American Chemical Society (ACS) National Meeting, Symposium on Environmental Applications and Ecological Implications of Nanotubes, Nanowires, and Fullerenes, Division of Environmental Chemistry, paper 528, March 25-29, 2012, San Diego, California.

(2) Changseok Han*, Amos Doepke, Wondong Cho, Armah A. de la Cruz, William R. Heineman, H. Brian Halsall, Vesselin N. Shanov, Mark J. Schulz, Vlassis Likodimos, Polycarpos Falaras and Dionysios D. Dionysiou, Carbon Nanotubes-based Biosensor for Detecting Cyanotoxins in Water. Poster Presentation at the 3rd International Conference from Nanoparticles and Nanomaterials to Nanodevices and Nanosystems (IC4N-3), June 26-30, 2011, Crete Island, Greece.

3. Students supported by the project

(1) Changseok Han
Ph.D. student, Environmental Engineering;

4. Brief description of notable awards or achievements resulting from the project

(1) 2012 *Certificate of Merit Award for First Paper Presentation*, American Chemical Society, Division of Environmental Chemistry, ACS 243rd meeting, March 25-29, San Diego.
(2) 2011 Best Poster Paper Award, 3rd International Conference from Nanoparticles and Nanomaterials to Nanodevices and Nanosystems, June 26-30, Crete, Greece.
(3) 2011 National Science Foundation Travel Award to attend the 3rd International Conference from Nanoparticles and Nanomaterials to Nanodevices and Nanosystems and the NSF Workshop; Participation in the Poster Competition, June 26-30, Crete, Greece.

5. Appendix List.

Appendix A-accepted paper. Analysis of the electrochemical oxidation of multi-walled carbon nanotube tower electrodes in sodium hydroxide.

Information Transfer Program Introduction

The Ohio Water Resources Center (WRC), at The Ohio State University, conducted a number of activities to transfer water related information to a wide range of state, federal, county, and municipal agencies, to the academic community, students, and to private citizens throughout Ohio. Specific activities included:

1) Preparation of information for the web site of the Ohio Water Resources Center and maintenance of the web site

2) Administration of a Special Water and Wastewater Treatment Grants Competition funded through the Ohio Water Development Authority - administration of the 104(B) In-State Competition and the 104(G) National Competitive Grants Program - encouraged investigators of projects funded through the Ohio WRC to develop publications in peer-reviewed journals and other outlets

3) Continued administrative support for the Water Management Association of Ohio (WMAO) and associated WMAO meetings, conferences, and division activities. Co-organization of quarterly OWRC-WMAO luncheon seminars.

4) Arranging and helping investigators of supported projects to disseminate their results in different newsletters published in the State of Ohio, such as Twine Line, Water Table and Buckeye Bulletin

5) Participation in the WiE (Women in Engineering) GROW program which focuses on introducing 8th grade girls to careers in various areas of engineering, including water resources and environmental engineering

6) Assisting in organizing Ohio River Basin Consortium for Research and Education conference in Athens, Ohio and leading the water and energy section

7) Responding to questions from the public regarding water resources issues in the state of Ohio

8) Creating a state wide database of water related investigators in Ohio Universities and sorting their research interests

USGS Summer Intern Program

None.

Student Support					
Category	**Section 104 Base Grant**	**Section 104 NCGP Award**	**NIWR-USGS Internship**	**Supplemental Awards**	**Total**
Undergraduate	1	0	0	2	3
Masters	4	0	0	1	5
Ph.D.	0	0	0	1	1
Post-Doc.	0	0	0	0	0
Total	5	0	0	4	9

Notable Awards and Achievements

2011OH291O "Development of Carbon Nanotube-based Biosensor for Monitoring Microcystin-LR in water": 2012 Certificate of Merit Award for First Paper Presentation, American Chemical Society, Division of Environmental Chemistry, ACS 243 Chemical Society, Division of Environmental Chemistry, ACS 243rd meeting, meeting, March 25-29, San Diego.

2011OH291O "Development of Carbon Nanotube-based Biosensor for Monitoring Microcystin-LR in water": 2011 Best post Paper Award, 3rd International Conference from Nanoparticles and Nanomaterials to Nanodevices adn Nanosystems, June 26-30, Crete, Greece.

2011OH291O "Development of Carbon Nanotube-based Biosensor for Monitoring Microcystin-LR in water": 2011 National Science Foundation Travel Award to attend the 3rd International Conference from Nanoparticles and Nanomaterials to Nanodevices and Nanosystems and the NSF Workshop

2011OH207B "Does Alum Addition Affect Benthic Communities and Metal and Nutrient Cycling? A Case Study from Grand Lake St. Marys, Ohio": A Phosphorus Budget for Grand Lake Saint Mary's, Ohio ($9,948) Funded by the Wright State University Research Council. C. R. Hammerschmidt (lead), A. J. Burgin, G. Nogaro.

2011OH207B "Does Alum Addition Affect Benthic Communities and Metal and Nutrient Cycling? A Case Study from Grand Lake St. Marys, Ohio": Phosphorus budget and benthic flux in eutrophic Grand Lake Saint Mary’s, Ohio ($750) Funded by Graduate Student Association, Wright State University. A. Taylor

Publications from Prior Years

1. 2009OH85B ("Early detection of membrane biofoulants using self-cleaning sensors") - Articles in Refereed Scientific Journals - Zaky A, I Escobar, C Gruden. June 2011. Studying the effect of feed water characteristics on the hydrophobicity of cellulose acetate ultrafiltraion membranes and its correlation to membrane morphology: A chemical force microscopy approach. In Modern Applications in Membrane Science and Technology (Hauserman, Ed.), ACS Publications. In Press.
2. 2009OH85B ("Early detection of membrane biofoulants using self-cleaning sensors") - Conference Proceedings - Mohahegh Motlagh, SA, A Zaky, C Gruden. July 2011. Multi-Scale Biofilm Characterization to Comprehend Early Stage Membrane Biofouling 2011 AEESP Education & Research Conference, University of South Florida, Tampa, FL.
3. 2009OH85B ("Early detection of membrane biofoulants using self-cleaning sensors") - Conference Proceedings - Mohahegh Motlagh SA, C Gruden. February 2011. Kinetic assessment of ultrafiltration membrane biofouling metabolic activity The 22nd Triennial Symposium on Advancements in Water & Wastewater, Ann Arbor, MI.
4. 2010OH160B ("THE INFLUENCE OF NATURAL ORGANIC MATTER ON BIOFILM GROWTH, CHLORINE EFFICACY, AND BY-PRODUCT FORMATION IN WATER DISTRIBUTION SYSTEMS") - Articles in Refereed Scientific Journals - Wang Zhikang, Youngwoo Seo (2011)Influence of Bacterial Extracellular Polymeric Substances (EPS) on Biosorption of Natural Organic Matter, Water Research
5. 2010OH160B ("THE INFLUENCE OF NATURAL ORGANIC MATTER ON BIOFILM GROWTH, CHLORINE EFFICACY, AND BY-PRODUCT FORMATION IN WATER DISTRIBUTION SYSTEMS") - Conference Proceedings - Zheng Xue and Youngwoo Seo, 2011, Quantitative Analysis of Biofilm Susceptibility against Mode Disinfectants, in Water Environmental Federation (WEF) Disinfection 2011 conference, Cincinnati, OH, 235-242.
6. 2010OH160B ("THE INFLUENCE OF NATURAL ORGANIC MATTER ON BIOFILM GROWTH, CHLORINE EFFICACY, AND BY-PRODUCT FORMATION IN WATER DISTRIBUTION SYSTEMS") - Conference Proceedings - Zhikang Wang and Youngwoo Seo (2011) Affect of Phenotypic Variation on Biosorption of Natural Organic Matter (NOM) Under Simulated Drinking Water Distribution System Conditions, Borchardt Conference, University of Michigan, Ann Arbor, MI, USA.
7. 2010OH160B ("THE INFLUENCE OF NATURAL ORGANIC MATTER ON BIOFILM GROWTH, CHLORINE EFFICACY, AND BY-PRODUCT FORMATION IN WATER DISTRIBUTION SYSTEMS") - Conference Proceedings - Zheng Xue and Youngwoo Seo (2011)Factors Modulating Biological Stability of Water in a Model Distribution System, Association of Environmental Engineering and Science Professors Education and Research Conference, Tampa, USA (Submitted).
8. 2010OH160B ("THE INFLUENCE OF NATURAL ORGANIC MATTER ON BIOFILM GROWTH, CHLORINE EFFICACY, AND BY-PRODUCT FORMATION IN WATER DISTRIBUTION SYSTEMS") - Conference Proceedings - Zheng Xue, Cyndee Gruden, Youngwoo Seo (2011) Efficacy of model disinfectant on biofilm and biofilm detachment, American Water Works Association Water Quality Technology Conference, Phoenix, Arizona, USA. (Submitted)
9. 2010OH160B ("THE INFLUENCE OF NATURAL ORGANIC MATTER ON BIOFILM GROWTH, CHLORINE EFFICACY, AND BY-PRODUCT FORMATION IN WATER DISTRIBUTION SYSTEMS") - Conference Proceedings - Wang Zhikang and Youngwoo Seo (2011) Biosorption of Natural Organic Matter in Water Distribution System, American Water Works Association Water Quality Technology Conference, Phoenix, Arizona, USA. (Submitted)
10. 2011OH205B ("The Constructed Wetland Dilemma: Nitrogen Removal at the Expense of Methane Generation?") - Conference Proceedings - Naor-Azrieli L, G Bohrer, W Mitsch. Collaborative research: Greenhouse gas balance of urban temperate wetlands. Oral presentation 5/2011. Annual

Meeting of the American Ecological Engineering Society, Ashville, NC.

11. 2010OH157B ("Nitrogen Removal by Microbial-Mediated Processes Under Hypoxic Conditions in Lake Erie") - Conference Proceedings - Lu X, LG Leff, D Bade, R Heath and X Mou. Denitrification overweigh the importance of Anammox in microbially-mediated nitrogen removal in Lake Erie. 2011 IAGLR Annual Conference on Great Lakes Research. May 2011, Duluth, MN, Invited Oral presentation.
12. 2009OH135B ("Exploring Spatial and Temporal Demand Aggregation on Transport Characteristics in Distribution System Modeling") - Articles in Refereed Scientific Journals - Yang X and DL Boccelli(2011). A Full-Scale Simulation Study of Stochastic Water Demands on Distribution System Transport. In preparation for Journal of Water Resources Planning and Management
13. 2009OH135B ("Exploring Spatial and Temporal Demand Aggregation on Transport Characteristics in Distribution System Modeling") - Conference Proceedings - Yang X and DL Boccelli(2010). A Full-Scale Simulation Study of Stochastic Water Demands on Distribution System Transport. 2010 Water Distribution Systems Analysis Symposium, Tucson, AZ
14. 2010OH157B ("Nitrogen Removal by Microbial-Mediated Processes Under Hypoxic Conditions in Lake Erie") - Conference Proceedings - Lu X, LG Leff, D Bade, R Heath, X Mou (2011) Denitrification overweigh the importance of Anammox in microbially-mediated nitrogen removal in Lake Erie. 2011 IAGLR Annual Conference on Great Lakes Research. May 2011, Duluth, MN, Invited Oral presentation.